

Forecasting Climate Policy Uncertainty: Evidence from the United States

Donia Beshar¹, Anirban Sengupta², Tanujit Chakraborty^{1,3}

¹ SAFIR, Sorbonne University Abu Dhabi, United Arab Emirates.

² Indian Institute of Management, Bodhgaya, India.

³ Sorbonne Center for Artificial Intelligence, Sorbonne University, Paris, France.

Abstract

Forecasting Climate Policy Uncertainty (CPU) is essential as policymakers strive to balance economic growth with environmental goals. High levels of CPU can slow down investments in green technologies, make regulatory planning more difficult, and increase public resistance to climate reforms, especially during times of economic stress. This study addresses the challenge of forecasting the US CPU index by building the Bayesian Structural Time Series (BSTS) model with a large set of covariates, including economic indicators, financial cycle data, and public sentiments captured through Google Trends. The key strength of the BSTS model lies in its ability to efficiently manage a large number of covariates through its dynamic feature selection mechanism based on the spike-and-slab prior. To validate the effectiveness of the selected features of the BSTS model, an impulse response analysis is performed. The results show that macro-financial shocks impact CPU in different ways over time. Numerical experiments are performed to evaluate the performance of the BSTS model with exogenous variables on the US CPU dataset over different forecasting horizons. The empirical results confirm that BSTS consistently outperforms classical and deep learning frameworks, particularly for semi-long-term and long-term forecasts.

Keywords: Macroeconomic forecasting, Climate Policy Uncertainty, Bayesian Structural time series, Google Trends

1. Introduction

Since the early 19th century, industrialization has served as the principal catalyst of economic growth across both developed and developing nations; by the close of the 20th century, this role had increasingly shifted to the service sector, which emerged as the dominant force driving global economic expansion (Grossman & Krueger, 1995; Chevallier, 2011). Although Gross Domestic Product (GDP) increased manifold in both developed and developing economies, this growth came at the cost of severe environmental degradation due to the emission of carbon dioxide (CO_2) and other harmful gases from industries and automobiles (Shahbaz, Balsalobre-Lorente & Sinha, 2019; Sobrino & Monzon, 2014; Dogan & Turkekul, 2016; Balsalobre-Lorente, Driha, Halkos & Mishra, 2022). Greenhouse gas (GHG) emissions have degraded the air quality index and threaten the ice caps in the Polar Regions (von Schneidemesser, Monks, Allan, Bruhwiler, Forster, Fowler,

Lauer, Morgan, Paasonen, Righi, Sindelarova & Sutton, 2015). The Kyoto Protocol¹ was adopted on 11th December 1997 to mitigate this issue. The Kyoto Protocol required developed economies to reduce their emissions by an average of 5.2% below 1990 levels during the commitment period. However, the Paris Agreement², signed in 2015, expanded the responsibility to both the developing and developed economies (Frayer, 2021). This broader commitment was also incorporated into the Sustainable Development Goals³ (SDGs), proposed by the United Nations in 2015, which call for global cooperation to balance environmental sustainability with economic progress. In particular, SDG 13 (Climate Action) and SDG 8 (Decent Work and Economic Growth) reflect the dual challenge of reducing emissions while sustaining development. The largest economies bear a particular responsibility to lead this transition and set an example for developing countries to follow by 2030.

The United States is the largest economy in the world and the second largest GHG emitter after China (Michaelowa & Michaelowa, 2015). Carbon emissions from the US account for 15% of the total global carbon emissions (Wang & Wang, 2019). Hence, if the US leads international emission reduction initiatives through climate change policies, it will greatly benefit the issue of climate change (Wu, Huang, Chen, Mao & Qi, 2022). During the period between 1990 and 2023, the gross emissions of US GHG have reduced by 3%. In 2020, due to COVID-19, there was a massive drop in GHG emissions. However, this sharp decline in GHG emissions reversed in 2021 and 2022 due to an economic rebound from the COVID-19-induced recession in 2020. In 2022, due to the burning of fossil fuels, CO_2 emissions in the US increased by 8% and 1% in comparison to 2020 and 2021, respectively. CO_2 emissions due to natural gas consumption increased by 5% in contrast to 2020. The rise and fall in the emission levels of GHGs⁴ are attributed to economic fluctuations and changes in fuel prices. The question that follows from this trend is whether the variation in GHGs can be attributed to changes in climate-change-related policies to accommodate economic recovery. *Do climate change policies vary with fluctuations in macroeconomic and financial cycle variables?* Economic indicators, including GDP, inflation, and unemployment, provide a broad picture of the state of the economy and serve as the foundation for government and central bank policies, such as interest rates, taxes, and transfers. GDP growth depends on industrial development, which results in employment and boosts national income, but at the expense of increased carbon emissions and threats to global warming due to reliance on non-renewable fossil-based sources of energy (Newell, Prest & Sexton, 2021; Pei, Chen, Li, Liang, Lin, Li, Yang, Bin & Dai, 2022). This trade-off between economic growth and environmental concerns also extends to unemployment, highlighting the challenges of balancing development with climate goals (Ng, Yui, Lau & Go, 2023). In addition, interest rates and inflation play an essential role in the formation of climate change policies (Akan, 2024). Expansionary monetary policies stimulate credit flows and the global financial cycle, thereby increasing global liquidity, particularly in emerging economies. Additionally, these flows drive industrial activities in the US, further exacerbating global warming risks. On the other hand, inflation discourages the adoption of cleaner, advanced technologies for

¹For more details, refer to the official UNFCCC page on the Kyoto Protocol: https://unfccc.int/kyoto_protocol.

²The Paris Agreement, adopted at COP21 in Paris, aimed to prevent the average global temperature from increasing by more than 2 degrees Celsius above preindustrial levels and to pursue efforts to limit the increase to 1.5 degrees Celsius. For more details, refer to the official UNFCCC page on the Paris Agreement: <https://unfccc.int/process-and-meetings/the-paris-agreement>.

³For more details, refer to the official UN page on the Sustainable Development Goals: <https://sdgs.un.org/goals>.

⁴US Environmental Protection Agency: <https://www.epa.gov/ghgemissions/sources-greenhouse-gas-emissions>.

industrial purposes. Further, governments and central banks across the world tend to focus more on economic recovery during recessions as a primary goal with fiscal stimulus and lower interest rates. At the same time, they relegate the policies to combat climate change as the secondary goal (Ide, 2020; Sultanuzzaman, Yahya & Lee, 2024; Sultanuzzaman et al., 2024; Gaies, 2025; Zhang, 2023). Concurrently, the Environmental Kuznets Curve theory states that economic growth and human capital development encourage the adoption of cleaner technologies (Kuznets, 1955). However, debates persist on how business cycles influence future climate risks and policy, necessitating an analysis of the ability of the US macroeconomic and financial cycle variables to forecast the US climate policy uncertainty (CPU).

To address this issue, this paper aims to forecast the US CPU based on other macroeconomic, financial cycle variables, and public sentiment indicators. This current study focuses on the US due to its central role in the global economic system. The US macroeconomic policies are vital in driving the global credit cycle, investments, and co-movements in the international financial variables. This substantiates the central role of the US in driving the global financial and business cycle (Miranda-Agrippino & Rey, 2020). A total of 137 exogenous variables covering a broad range of US macroeconomic and financial cycle indicators, along with Google Trends data (depicting economic sentiments), are considered to forecast the US CPU. To measure uncertainties related to climate policy, we consider the US CPU index developed by Gavriilidis, 2021. This CPU index measures the fluctuations of US climate policies. The CPU index is based on relevant climate policy reports from eight significant newspapers: the Wall Street Journal, Boston Globe, Los Angeles Times, Chicago Tribune, New York Times, Tampa Bay Times, Miami Herald, and USA Today. This current study of US CPU data is characterized not only by a limited number of observations and many exogenous time series, but also by temporal dependence. Most econometric and machine learning time series forecasting models are well-suited to handling only a very limited number of exogenous variables in macroeconomic analysis within policy institutions. To fill this gap, this study builds the Bayesian Structural Time Series (BSTS) model to forecast the US CPU.

The BSTS model provides a dynamic and well-structured methodology for policymakers to better understand the uncertainty of climate-related policies stemming from economic changes and the financial cycle. Bayesian models, which are underexplored in this domain, are especially suited for CPU forecasting as a result of their flexibility in scenarios with high uncertainty and their ability to incorporate macroeconomic and financial cycle variables. Using a combination of causality analysis methods such as Granger causality, transfer entropy, cross-correlation, and wavelet coherence analysis, this study demonstrates that the CPU index is strongly affected by both US economic and financial conditions. To compare the performance of BSTS in comparison with benchmark statistical and deep learning models, an experimental validation is performed via a forecast cross-validation technique. The experimental results demonstrate that the BSTS model provides the most accurate CPU index forecasts, outperforming other forecasting methodologies for varying forecast horizons. Also, the BSTS model highlights several key macroeconomic and financial variables in forecasting the CPU such as Cyclically Adjusted Price to Earnings ratio (a stock market valuation metric), Business Conditions Index (a measure of economic activity), Composite Leading Indicator (economic turning points in business cycles), New Private Housing Permits in the Northeastern US (indicating housing market activity), and UEMP15OV (unemployed individuals for 15 weeks and over). This feature importance mechanism of the BSTS model provides insights

to policymakers involved in climate change and macroeconomists for formulating economic policies that take into consideration the issue of climate change. Unlike classical time series models, BSTS is particularly well-suited for forecasting in complex economic environments due to its capacity to incorporate latent state components, prior information, and handle high-dimensional datasets. The model is further updated based on the observed data, thus providing accurate forecasts even under circumstances of scarce or uncertain data (West & Harrison, 1997). This makes it highly effective in capturing structural shifts and persistent volatility inherent in the CPU series. In addition, the use of the Local Projections method for impulse response analysis offers a robust alternative to traditional vector autoregression (VAR) models, providing clearer insights into the dynamic effects of macroeconomic shocks on CPU. This study also integrates measures of public sentiment using data from Google Trends, thereby capturing real-time shifts in public concern related to climate policy. This targeted identification of influential variables enables more effective policy design and more timely intervention, with implications for both economic stabilization and climate governance.

The rest of the paper is organized as follows: Section 2 provides a brief literature review on climate change and macroeconomic policy making. This is followed by Section 3 discussing the details of the Bayesian Structural Time Series (BSTS) model. Section 4 presents the data used in the analysis and reports the empirical results of forecasting methods. Then, Section 5 focuses on the feature importance plot and impulse response analysis. Finally, the Sections 6 and 7 provide policy implications and conclude the paper, respectively.

2. Literature Review

The Climate Policy Uncertainty index refers to the unpredictability of the legislative decisions for actions to reduce the effects of climate change. It plays a role in corporate decision-making and financial planning, as industries sensitive to policy fluctuation and regulations, such as energy, manufacturing, and finance, may be hesitant to commit to expensive or long-term ventures in the absence of policy directions (Liang, Umar, Ma & Huynh, 2022; Xu, Li, Yan & Bai, 2022). Ambiguity and frequent changes in policy design and implementation lead industries, mainly those with capital-intensive investments, to postpone or decrease investment due to the uncertainty of returns. Such hesitation may slow the adoption of green technologies and correspondingly delay progress toward emission reduction goals (Yang, Dong & Liang, 2024; Raza, Khan, Benkraiem & Guesmi, 2023). Given the global need for vast investments in low-carbon infrastructure such as renewable energy, CPU becomes a significant deterrent to the private and public sectors (Berestycki, Carattini, Dechezleprêtre & Kruse, 2022; Liang et al., 2022). Further, Matzner & Steininger, 2024 investigated the impact of carbon pricing on investment decisions across diverse European companies, using data from 1.2 million firms and focusing on specific instances where carbon policies changed unexpectedly. This study revealed that increases in carbon prices tend to dampen corporate investment. However, this effect is more pronounced in companies and sectors that are less reliant on carbon-intensive practices. Moreover, in industries characterized by high demand sensitivity, carbon price hikes lead to broader negative effects extending beyond investment to declines in sales, employment, and cash flow.

A vast amount of research has investigated the effects of CPU on various economic indicators

and investment behaviours. For instance, [Yang et al., 2024](#) have investigated the effect of CPU on economic cycles; their results indicate that positive CPU index shocks are associated with economic downturns, which subsequently affect variables such as GDP growth and unemployment rates. [Xu et al., 2022](#) analyzed the predictive power of CPU on returns in the renewable energy market and found a significant correlation between high CPU levels and increased market volatility. In a closely related study, [Liang et al., 2022](#) demonstrated that CPU contributes meaningfully to volatility forecasting in the renewable energy field, thereby highlighting the economic relevance of CPU. Additionally, the recent studies by [Arouri, Gomes & Pijourlet, 2025](#); [Xing, Liu, Zhu & Deng, 2024](#); and [Yousaf, Mohammed, Yousaf & Serret, 2025](#) have found that the CPU can impact return on financial assets, sovereign credit risk, and the US economic cycle. [Bauer, Offner & Rudebusch, 2023](#) investigated how carbon policies impact stock returns by studying the EU Emissions Trading System (ETS) and high-frequency data on 2000 European companies. This study observed that increases in carbon prices, especially when unexpected, lead to lower stock returns, particularly for companies with high carbon emissions. Even companies not directly involved in the ETS experienced this effect, indicating investors were concerned about the broader economic shift toward reducing carbon emissions. [Ghani, Zhu, Qin & Ghani, 2024](#) examined the ability of the environmental, social, and governance (ESG) index alongside the CPU index to predict volatility in the US stock market through the Markov-regime GARCH-MIDAS model. Their findings from out-of-sample tests indicated that information regarding ESG and CPU is valuable for forecasting volatility in the US stock market. Importantly, the ESG index emerged as a significantly stronger predictor for estimating volatility. [Naifar, 2024](#) noted that the US CPU affected the spillover of sovereign credit risk among the G20 nations, highlighting the critical role of climate policy variables in determining international financial dynamics. Their study examined data on credit default swaps to understand the spillover risk dynamics among them using a TVP-VAR approach and found a link between climate uncertainty and the spread of credit default risk, especially in G20 countries that are highly financially connected. Their findings suggest that it is important for G20 countries to work together on clear climate policies to keep their financial systems stable. Also, CPU have been found to profoundly impact the stock prices of clean energy companies and commodities. [Iqbal, Bouri, Shahzad & Alsagr, 2024](#) examined the asymmetric impact of Chinese CPU on clean energy stocks' prices using NARDL daily data during the period between February 2015 and December 2022. The findings suggest that higher Chinese CPU decreases the prices of carbon emission allowances and increases the ESG index over the long term. However, the study failed to find any evidence of asymmetric co-integration between the uncertainty of Chinese climate policy and the oil and gas stock index. Recently, [Arouri et al., 2025](#) observed that the CPU plays an important role in determining the sensitivity of the GCC countries' stock market returns to oil price shocks. The CPU is negatively moderating the link between GCC stock market returns and oil price shocks. [Wu & Hu, 2024](#) developed the CPU indices of 21 economies and 3 global indices to study their impact on long-term green and sovereign bond volatility and their correlation. By applying the extended GARCH-MIDAS-CPU and DCC-MIDAS-CPU models, they found that CPU significantly impacted the volatility of sovereign bonds after the Paris Agreement. These studies have predominantly focused on the impact of CPU on macroeconomic variables, indicating a notable gap in the literature regarding the reverse relationship: *How macroeconomic and financial cycle variables influence climate policy uncertainty?* This gap is emerging despite an established positive relationship between long-term economic growth theory and climate change ([Fankhauser & Tol, 2005](#); [Narayan, Saboori & Soleymani, 2016](#); [Lu, Ma & Feng, 2024](#); [Mokni,](#)

Zaier, Youssef & Jabeur, 2024). Motivated by the above discussion, this study aims to fill the gap by focusing on the impact of short-term macroeconomic variables and financial markets on climate policy uncertainty, which is severely lacking.

The motivation for forecasting the CPU using the macroeconomic and financial cycle variables is further strengthened by the debate in the climate change-business cycle literature. These discussions highlight that governments worldwide, including the US, tend to prioritize economic recovery during recessions as a primary goal, often relegating climate change mitigation policies to a secondary goal (Layzer, 2011; Heutel, 2012; Ide, 2020; Zhang & Chiu, 2020; Annicchiarico, Carattini, Fischer & Heutel, 2022; Sultanuzzaman et al., 2024; Yeganeh, McCoy & Schenk, 2020; Bumann, 2021). During recessions, the central banks and governments pursue expansionary fiscal policy, such as reducing interest rates and tax cuts, to increase consumption in the economy (Halkos & Paizanos, 2016; Wu, Yang & Chen, 2024). Adebayo, Kartal, Ağa & Al-Faryan, 2023 noted that post-COVID fiscal stimulus increased the CO_2 emissions from China and MINT (Mexico, Indonesia, Nigeria, and Turkey) countries, respectively. This trend is on similar lines to the increase of CO_2 emissions in the US during 2022. This raises the question of whether we can attribute this increase in CO_2 emissions and related climate policy uncertainties in the US during 2022 to the policies that targeted faster post-pandemic recovery in the country? During recessions, the priorities of governments and central banks shift to emphasize economic recovery, thereby making climate policies a second priority (Obani & Gupta, 2016; Shum, 2012). Public perception plays a significant role in shaping these shifting priorities, as the public concentrates on recovery, often viewing climate change as an obstacle (Drews & Van den Bergh, 2016; Ge & Lin, 2021). As a result, there is a diminished societal focus on developing a green economy in both developed and developing economies. This makes the trade-off between economic policies for recovery and climate change a politically sensitive issue (Danisman, Bilyay-Erdogan & Demir, 2025). Recently, Gaies, 2025 noted that the US financial stress impacts the CPU in China. This gives a strong indication that short-run macroeconomic policies of the US might have an impact on its CPU.

To address the issue of whether uncertainty related to climate policies is dependent on the state of the business and financial cycle, we forecast the US CPU using the BSTS model, incorporating a selected subset of the 137 US macroeconomic and financial cycle variables identified through causal analysis, along with Google Trends data to reflect public sentiment. The BSTS model has the ability to model complex structural changes in the nonstationary time series data having a large number of causal variables. This makes the BSTS model very effective in modeling financial and macroeconomic data that exhibit seasonality, high volatility, and regime-changing behaviour. These issues of macro-financial data can be handled by combining the state-space models with Bayesian inference to decompose the time series data into seasonal, trend, and regression components. This decomposition enhances forecasting accuracy (Scott & Varian, 2014). Koop, Korobilis et al., 2010 applied BSTS to predict the macro-financial and economic indicators having a high degree of uncertainty, thereby enhancing the decision-making in financial markets. Applying techniques like BSTS can isolate the policy effects from confounders like macroeconomic trends or climate variability (Brodersen, Gallusser, Koehler, Remy & Scott, 2015). The efficacy of the BSTS model can be extended to study the climate policy analysis that involves issues such as renewable energy or carbon taxes, by estimating causal impacts with counterfactual analysis. Its inherent flexibility in handling structural breaks and missing data makes it a very suitable method for long-term

time series forecasting (West & Harrison, 1997). Hence, BSTS can be very applicable in long-term climate risk modeling.

3. Methodology

The Bayesian time series model used for analysis is developed using the Bayesian Structural Time Series model given by Scott & Varian, 2014. BSTS offers a flexible approach for forecasting time series data that extends the classical structural time series model by incorporating Bayesian inference to jointly estimate the model parameters and unobserved components. First, the observed series y_t is decomposed into latent components such as trends, seasonal fluctuations, and the influence of external covariates. Each component is specified within a state-space formulation, which provides a systematic way to model their evolution over time. The Bayesian framework enables the inclusion of prior knowledge, which is beneficial in producing forecasts through the posterior distribution. This combination makes BSTS particularly useful in economic forecasting problems, where interpretability and the integration of diverse economic and sentiment indicators are crucial. The BSTS framework relies on the state-space representation, where the observed time series y_t is associated with an unobserved state vector α_t . This formulation uses the idea that the observable data are generated by latent processes evolving over time. The general form of a state-space model can be expressed as:

$$\begin{aligned} y_t &= Z_t^\top \alpha_t + \epsilon_t, & \epsilon_t &\sim \mathcal{N}(0, H_t) \\ \alpha_{t+1} &= T_t \alpha_t + R_t \eta_t, & \eta_t &\sim \mathcal{N}(0, Q_t), \end{aligned} \tag{1}$$

where y_t denotes the observed time series, α_t represents the latent state vector encompassing the unobserved components of the model. The matrices Z_t and T_t are the observation and transition matrices, respectively. The observation matrix Z_t links the unobserved states to the observed data, while the transition matrix T_t describes how the unobserved states change over time. The terms ϵ_t and η_t are independent and identically distributed Gaussian noise processes with covariance matrices H_t and Q_t , respectively, reflecting observation and state uncertainties. We consider the observation noise covariance H_t to be a positive scalar, denoted by σ_ϵ^2 , following the specification in Scott & Varian, 2014.

The BSTS framework allows modeling various components to capture different features of a time series. Commonly used components include:

1. Local Level: This component models the series level as a random walk, allowing it to evolve gradually and unpredictably over time by adding small random changes at each step:

$$\mu_t = \mu_{t-1} + u_t, \quad u_t \sim \mathcal{N}(0, \sigma_u^2).$$

2. Local Linear Trend: This extends the local level by adding a slope term δ_t to account for trends that can change smoothly:

$$\mu_t = \mu_{t-1} + \delta_{t-1} + u_t, \quad \delta_t = \delta_{t-1} + v_t, \quad v_t \sim \mathcal{N}(0, \sigma_v^2).$$

3. Autoregressive Process: This component introduces an autoregressive structure of order p , denoted $\text{AR}(p)$, for some positive integer p . In an $\text{AR}(p)$ process, the current state depends on its previous p lagged observations:

$$\mu_t = \sum_{i=1}^p \phi_i \mu_{t-i} + \tilde{u}_t, \quad \tilde{u}_t \sim \mathcal{N}(0, \sigma_{\tilde{u}}^2).$$

4. Seasonal: This component captures recurring seasonal patterns by including a seasonal effect τ_t modeled through dummy variables. The parameter S denotes the length of the seasonal cycle. The seasonal component evolves according to the equation below, which imposes the constraint that seasonal effects sum to zero over one full cycle of length S .

$$\tau_t = - \sum_{s=1}^{S-1} \tau_{t-s} + w_t, \quad w_t \sim \mathcal{N}(0, \sigma_w^2).$$

5. Regression: This component allows the model to include external covariates x_t with coefficients β . The model employs a spike-and-slab prior to select relevant predictors by shrinking the coefficients of irrelevant variables toward zero with high probability. The full observation equation is:

$$y_t = \mu_t + \tau_t + \beta^\top x_t + \epsilon_t,$$

where $\epsilon_t \sim \mathcal{N}(0, \sigma^2)$ is the observation noise.

By combining these components, the BSTS model can flexibly capture a wide range of patterns and behaviours, including structural changes, gradual shifts, periodic fluctuations, and the influence of external covariates, found in macroeconomic time series data.

3.1. Prior Specification

To handle high-dimensional data with a large number of potential exogenous predictors, the BSTS model employs a spike and slab prior to induce sparsity by effectively setting most regression coefficients to zero while allowing a subset to vary (Varian, 2014). This is relevant for CPU forecasting due to the strong association between CPU and many macroeconomic and financial cycle variables, which can be considered as exogenous predictors. This approach begins by introducing an indicator variable γ_k , which denotes whether predictor x_k is included in the model:

$$\gamma_k = \begin{cases} 1, & \text{if } \beta_k \neq 0 \\ 0, & \text{if } \beta_k = 0, \end{cases}$$

where β_k is the coefficient of predictor x_k . Then, we define β_γ as the vector of regression coefficients corresponding to predictors with $\gamma_k = 1$. The joint prior over the coefficients β , indicator vector γ , and observation noise variance σ_ϵ^2 , namely the ‘‘spike and slab’’ prior, can be written as:

$$p(\beta, \gamma, \sigma_\epsilon^2) = p(\beta_\gamma | \gamma, \sigma_\epsilon^2) p(\sigma_\epsilon^2 | \gamma) p(\gamma).$$

The marginal prior $p(\gamma)$, often referred to as the “spike”, assigns high probability to zero coefficients for irrelevant predictors, thereby encouraging sparsity. For computational convenience, each γ_k is typically assumed to follow an independent Bernoulli distribution:

$$\gamma \sim \prod_{k=1}^K \pi_k^{\gamma_k} (1 - \pi_k)^{1-\gamma_k},$$

where π_k represents the prior inclusion probability of predictor x_k . In practice, all π_k are set to a common value $\pi = \frac{\tilde{p}}{K}$, defined as the expected model size, with \tilde{p} being the expected number of nonzero predictors and K being the total number of predictors. The “slab” part of the prior corresponds to the conditional conjugate priors on the included coefficients and the variance, $p(\beta_\gamma | \sigma_\epsilon^2, \gamma)$ and $p\left(\frac{1}{\sigma_\epsilon^2} | \gamma\right)$, respectively. They are modeled as:

$$\beta_\gamma | \sigma_\epsilon^2, \gamma \sim \mathcal{N}\left(b_\gamma, \sigma_\epsilon^2 (\Omega_\gamma^{-1})^{-1}\right), \quad \frac{1}{\sigma_\epsilon^2} | \gamma \sim \text{Gamma}\left(\frac{\nu}{2}, \frac{ss}{2}\right),$$

where b_γ represents the prior mean vector, Ω_γ^{-1} is a symmetric matrix corresponding to $\gamma_k = 1$, and ss and ν denote the expected coefficient of variation R^2 from the regression and the prior sample size, respectively. The precision matrix Ω_γ^{-1} is defined as $\Omega_\gamma^{-1} = \kappa (\omega X^\top X + (1 - \omega) \text{diag}(X^\top X)) / n$, where X is the design matrix, n is the total number of observations, and κ represents the number of significance observations on the prior mean $b_\gamma = 0$, with $\omega = \frac{1}{2}$ and $\kappa = 1$, following [Scott & Varian, 2014](#). This formulation enables the model to select the most relevant predictors for the observed time series while excluding irrelevant exogenous predictors.

3.2. Posterior Distribution

In Bayesian inference, the posterior distribution reflects updated beliefs about model parameters after incorporating the observed data. This is especially valuable in economic applications, where uncertainty and prior knowledge play a critical role in inference and forecasting. In order to derive the posterior distribution, we first define θ as the set of model parameters, excluding the regression coefficients β and the observation noise variance σ_ϵ^2 . The posterior distribution $p(\theta | y)$ is given by using Bayes’ theorem as:

$$p(\theta | y) = \frac{p(y | \theta) p(\theta)}{p(y)},$$

where $p(y | \theta)$ is the likelihood of the observed data given the parameters θ , $p(\theta)$ is the prior belief about the parameters before observing the data, and $p(y)$ is the marginal likelihood, acting as a normalizing constant, obtained by integrating out all the parameters. In order to facilitate posterior inference, the observed series is transformed to separate the contributions of the latent state α_t from those of the covariates by defining $\mathbf{y}_t^* = y_t - Z_t^{*\top} \alpha_t$, where $Z_t^{*\top}$ is the observation matrix from Eqn. (1) with the regression term $\beta^\top x_t$ excluded. Given a specific predictor inclusion vector γ , the conditional posterior distributions for the regression coefficients β_γ and noise variance σ_ϵ^2 are:

$$\beta_\gamma | \sigma_\epsilon^2, \gamma, \mathbf{y}^* \sim \mathcal{N}(\tilde{\beta}_\gamma, \sigma_\epsilon^2 (V_\gamma^{-1})^{-1}), \quad \frac{1}{\sigma_\epsilon^2} | \gamma, \mathbf{y}^* \sim \text{Gamma}\left(\frac{N}{2}, \frac{SS_\gamma}{2}\right).$$

Following the specifications of [Scott & Varian, 2014](#), the matrix $V_\gamma^{-1} = (X^\top X)_\gamma + \Omega_\gamma^{-1}$. The posterior mean of the regression coefficients for the selected variables $\tilde{\beta}_\gamma = (V_\gamma^{-1})^{-1} (X_\gamma^\top \mathbf{y}^* + \Omega_\gamma^{-1} b_\gamma)$. The sample size N combines the observed sample size n and the prior sample size ν , i.e., $N = n + \nu$, and the adjusted sum of

squares: $SS_\gamma = ss + \mathbf{y}^{*\top} \mathbf{y}^* + b_\gamma^\top \Omega_\gamma^{-1} b_\gamma - \tilde{\beta}_\gamma^\top V_\gamma^{-1} \tilde{\beta}_\gamma$. Intuitively, these expressions update the prior distribution of the regression coefficients β_γ by integrating information from the observed data, represented by $X^\top X$, with prior knowledge encoded in the precision matrix Ω_γ^{-1} and mean vector b_γ . The resulting posterior reflects a weighted balance between the data likelihood and prior beliefs. Subsequently, the marginal posterior distribution for γ , which determines which predictors are included, is given by:

$$\gamma | \mathbf{y}^* \sim C(\mathbf{y}^*) \frac{|\Omega_\gamma^{-1}|^{\frac{1}{2}} p(\gamma)}{|V_\gamma^{-1}|^{\frac{1}{2}} SS_\gamma^{\frac{N}{2}-1}},$$

where $C(\mathbf{y}^*)$ is a normalizing constant that is independent of γ . The posterior distribution of the BSTS model is difficult to compute explicitly because of its high dimensionality and highly structured dependencies. However, it can be approximated using a Markov Chain Monte Carlo algorithm by the following steps:

1. Sample the latent state α from $p(\alpha | y, \theta, \beta, \sigma_\epsilon^2)$ using the simulation smoother of [Durbin & Koopman, 2002](#). This step accounts for the time-varying unobserved components such as trend and seasonality.
2. Sample the parameters θ from $p(\theta | y, \alpha, \beta, \sigma_\epsilon^2)$, updating beliefs about the components.
3. Sample the regression coefficients β and variance σ_ϵ^2 from a Markov chain with stationary distribution $p(\beta, \sigma_\epsilon^2 | y, \alpha, \theta)$.

Setting $\phi = (\theta, \beta, \sigma_\epsilon^2, \alpha)$, the procedure could be iterated to produce samples $\phi^{(1)}, \phi^{(2)}, \dots$, which converge in distribution to the true posterior $p(\phi | y)$ ([Scott & Varian, 2014](#)).

4. Data and Results

4.1. Dataset

The US CPU index series used in this analysis, sourced from the Economic Policy Uncertainty website (https://www.policyuncertainty.com/climate_uncertainty.html/), is a monthly time series running from April 1987 to June 2023, with 435 observations. Initially, we started with 137 variables predominantly from the FRED-MD dataset ([McCracken & Ng, 2016](#)) depicting the US's macroeconomic and financial cycle variables, which were considered to examine their potential influence on the predictive models. These variables include key macroeconomic indicators such as GDP, inflation, unemployment rates, labor market metrics, credit conditions, and financial indices, providing a comprehensive view of the US economy. [McCracken & Ng, 2016](#) proposed presenting this large macroeconomic dataset quarterly. Later, they introduced a monthly version of the dataset. Further details about the transformations applied to this data to ensure robustness are provided in [McCracken & Ng, 2016](#) and summarized in [Table 1](#). This dataset has been earlier used to forecast economic policy, commodity risk premiums, and US GDP in [Carriero, Clark & Marcellino, 2018](#); [Rad, Low, Miffre & Faff, 2023](#); and [Moramarco, 2024](#). To address the risk of overfitting and identify the most relevant predictors, the study employs a combination of four causal inference methodologies: Transfer Entropy, Granger Causality, Cross-Correlation, and Wavelet Coherence. These techniques are used to evaluate the directional influences and temporal dependencies between each macro-financial variable and the CPU index. As a result, the number of macroeconomic and financial cycle variables is reduced to 60, retaining only those with statistically significant influence on the CPU index. A comprehensive explanation of the applied methodologies and a detailed presentation of the resulting causal inferences are provided in the [Appendix 8.1](#). Alongside the macroeconomic and financial cycle variables, sentiment indicators were

constructed from Google Trends data using search terms relevant to CPU, such as “climate policy”, “climate action”, “climate news”, “renewable energy”, and “green technology”. Causality analyses confirm a significant association between the selected Google Trends search terms and the US CPU index. The results of these analyses are also provided in Appendix 8.1.5. These sentiment measures complement the macro-financial variables by capturing public attention and concerns surrounding climate policy developments, and can thereby enrich the explanatory power of the forecasting models.

Table 1: Lists the financial cycle variables, where x_t denotes the respective time series and x_{t-k} denotes the respective time series with k lags. Detailed descriptions of the sources are available at [Moramarco, 2024](#).

Variable	Label	Source	Transformation
Business Confidence Index	bci	OECD	x_t
Composite Leading Indicator	cli	OECD	x_t
Real S&P500 Index Growth	sp500	Shiller	$\ln(x_{t-1})-\ln(x_{t-4})$
Cyclically Adjusted Price/Earnings ratio	cape	Shiller	$\ln(x_t)$
Real Credit Growth	cred	Fred	$\ln(x_{t-1})-\ln(x_{t-4})$
Credit/GDP ratio	cred_gdp	BIS	x_t
Real house price growth	hpi	Shiller	$\ln(x_{t-1})-\ln(x_{t-4})$
Cyclically Adjusted Price/Rent ratio	capr	FRED	$\ln(x_t)$
Household real mortgage debt growth	mortg	FRED	$\ln(x_{t-1})-\ln(x_{t-4})$
Household Mortgage/Income ratio	mortg_inc	FRED	x_t
Private residential fixed investment/GDP ratio	prfi_gdp	FRED	x_t
Personal Interest Payments/Income ratio	pip_inc	FRED	x_t
Chicago Fed national financial condition index	nfcf	FRED	x_t

4.2. Descriptive and Exploratory Analysis

The summary statistics and global characteristics of the training CPU series, running from April 1987 to June 2021, are presented in Tables 2 and 3, respectively. Table 2 presents key descriptive measures, including the coefficient of variation (CoV), which measures variability relative to the mean, and entropy, which captures the complexity and uncertainty inherent in the distribution of the CPU index. Table 3 reports key time series properties including distributional shape (skewness and kurtosis), nonlinearity, seasonality, and long-term memory ([Hyndman & Athanasopoulos, 2018](#)). The skewness and kurtosis values indicate a right-skewed distribution with heavier tails, which reflects asymmetry and a higher likelihood of extreme values. Nonlinearity was evaluated using Tsay’s and Keenan’s one-degree tests, both of which confirm that the CPU index series exhibits significant nonlinear behaviour. Seasonality was detected using the Ollech and Webel test, and the Kwiatkowski-Phillips-Schmidt-Shin (KPSS) test confirmed that the series is nonstationary. Finally, the Hurst exponent provides evidence of the presence of long-range dependence in the CPU series. This characteristic can be further examined through autocorrelation analysis. The autocorrelation function (ACF) and partial autocorrelation function (PACF) plots in Fig. 1 reveal a pronounced autocorrelation structure, indicating that past values of the CPU series exert a persistent influence on future values across multiple lags.

Given the presence of seasonality and the pronounced autocorrelation structure, there is a clear motivation to adopt a modeling approach that explicitly accounts for structural components. Fig. 1 further supports this by presenting the STL (Seasonal and Trend decomposition using Loess) decomposition of the CPU index, which separates the series into trend, seasonal, and remainder components. This decomposition

not only offers valuable insight into the underlying temporal dynamics but also justifies the use of the BSTS model. Although BSTS does not explicitly model long-range dependence, its flexible framework captures trends and seasonal patterns, thus enabling an accurate representation of the complex evolution of CPU over time. In addition, the time series plot portrayed in Fig. 1 further reveals significant variability in the CPU index, marked by periods of intensified uncertainty in policy direction. The plot depicts a clear upward trend, suggesting an increase in climate-related policies over time. While the trend is generally pretty stable, noticeable spikes do correspond with major world events or changes in climate policy. A comparable pattern can be observed in Fig. 2, where fluctuations in search interest closely mirror some of the variations in the CPU series. This alignment suggests that Google Trends data could aid in forecasting the CPU index.

Table 2: Presents the summary statistics of the training US CPU index series.

Min Value	Q1	Median	Mean	Q2	Max Value	CoV	Entropy
28.162	63.563	84.166	94.876	108.046	346.612	49.777	6.019

Table 3: Presents the statistical characteristics of the training US CPU index series.

Skewness	Kurtosis	Linearity	Seasonality	Stationarity	Long Range Dependence
1.863	4.531	Nonlinear	Seasonal	Nonstationary	0.780

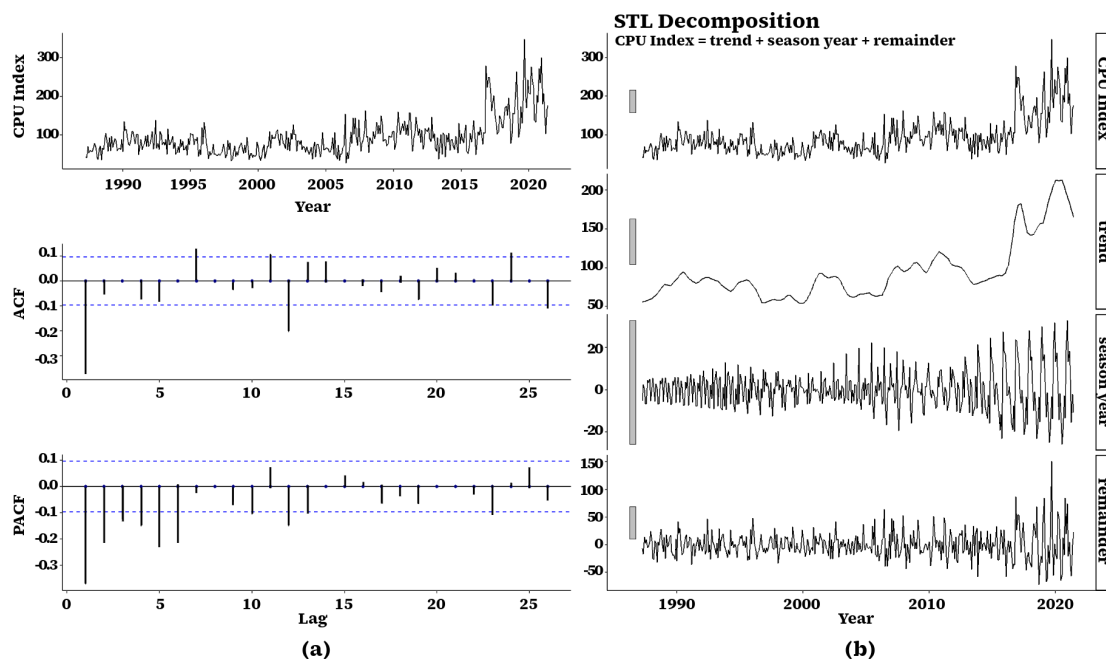


Figure 1: Illustrates (a) the training US CPU index series (April 1987 to June 2021) along with its ACF and PACF plots, and (b) STL decomposition of the series into trend, seasonal, and remainder components.

4.3. Modeling and Results

We evaluated the effectiveness of the BSTS model by comparing its performance against benchmark statistical and deep learning models. The experiments involved forecasting across five time horizons: 1-month-ahead, 3-month-ahead, 6-month-ahead, 12-month-ahead, and 24-month-ahead, to demonstrate the adaptability of the BSTS model. This section is organized as follows: Subsections 4.3.1 and 4.3.2 provide concise overviews of the baseline models and the evaluation metrics, respectively. Subsection 4.3.3 details

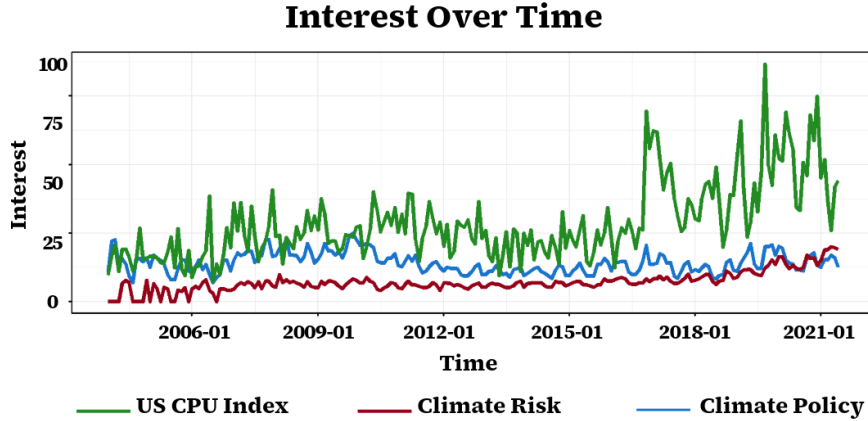


Figure 2: Portrays the interest in the search terms “climate policy” and “climate risk” from January 2004 to June 2021, plotted alongside the US CPU index. The three series exhibit similar temporal patterns. Data sourced from Google Trends: <https://trends.google.com/trends?geo=&hl=en-GB>.

the experimental results and benchmark comparisons. Finally, Subsection 4.3.4 discusses the statistical significance of the forecasts.

4.3.1. Baseline Models

The performance of the BSTS model was evaluated against several statistical and deep learning models. The comparison was conducted using the following competitive frameworks:

- *Autoregressive Integrated Moving Average with exogenous variables* (ARIMAX) model captures linear dependencies by integrating: an autoregressive (AR) component, differencing (I), and a moving average (MA) component (Box & Pierce, 1970). In this framework, initially, differencing of order d is applied to obtain a stationary series. Then, the AR component models p -lagged values of the series, while the MA component models q -lagged residuals. The coefficients are estimated by minimizing the Akaike Information Criterion (AIC).
- *Autoregressive Fractionally Integrated Moving Average with exogenous variables* (ARFIMAX) model extends the traditional ARIMA model by allowing the differencing parameter d to range between $(0, 0.5)$, enabling ARFIMA(p, d, q) to effectively handle time series exhibiting long-range dependencies, where correlations decay slowly over time (Granger & Joyeux, 1980).
- *Autoregressive Neural Network with exogenous variables* (ARNNX) model generalizes the feed-forward neural network structure to handle autoregressive time series processes (Faraway, 1998). In the ARNN(p, k) model, p -lagged values are fed into the input layer and processed by k neurons in the hidden layer. Commonly, k is set to $\lfloor \frac{p+1}{2} \rfloor$. The model is first initialized with random values and trained using the gradient descent back-propagation algorithm (Rumelhart, Hinton & Williams, 1986); thus achieving robust learning and preventing overfitting (Hyndman & Athanasopoulos, 2018).
- *Neural Basis Expansion Analysis for Time Series with exogenous variables* (NBeatsX) framework consists of multiple blocks, each comprised of two main layers (Oreshkin, Carpov, Chapados & Bengio, 2019). The first layer captures and models the general patterns in the data, while the second layer refines the forecasts obtained from the first layer by re-modeling the residuals. This iterative approach improves the overall forecasting accuracy.

- *Neural Hierarchical Interpolation for Time Series with exogenous variables* (NHITSX) is an extension of the NBeats framework by imposing a hierarchical structure. Similar to NBeats, NHITS consists of a sequence of blocks, albeit with a hierarchical design to better capture complex dependencies and relationships in the data (Challu, Kang, Santos, Montero-Manso & Hyndman, 2023).
- *Decomposition-based Linear model with exogenous variables* (DLinearX) decomposes the input time series into trend and seasonal components via moving average. Each component then goes through an independent linear layer, and the sum of their results is the final forecast. This method provides better performance by dealing with the trends in the data (Zeng, Liu, Li, Wei & Hong, 2023).
- *Normalization-based Linear model with exogenous variables* (NLinearX) normalizes the input time series by subtracting its last value before passing it through a linear layer; then, the processed output has the subtracted value added back to produce the final forecast. This normalization technique is specially devised to cope with distribution shifts between the training and testing datasets (Zeng et al., 2023).

4.3.2. Evaluation Metrics

Five evaluation metrics are adopted to assess the performance of the competing models in forecasting the CPU index across the five horizons. These metrics are Root Mean Squared Error (RMSE), Mean Absolute Error (MAE), Mean Absolute Scaled Error (MASE), Mean Absolute Percentage Error (MAPE), and Symmetric Mean Absolute Percentage Error (SMAPE). The mathematical formulation of these metrics is given by:

$$\begin{aligned} \text{RMSE} &= \sqrt{\frac{1}{h} \sum_{t=1}^h (y_t - \hat{y}_t)^2}; & \text{MASE} &= \frac{\sum_{t=1}^h |\hat{y}_t - y_t|}{\frac{h}{T-1} \sum_{t=2}^T |y_t - y_{t-1}|}; & \text{MAE} &= \frac{1}{h} \sum_{i=1}^h |y_i - \hat{y}_i|; \\ \text{MAPE} &= \frac{1}{h} \sum_{t=1}^h \frac{|\hat{y}_t - y_t|}{|y_t|} \times 100\%; & \text{SMAPE} &= \frac{1}{h} \sum_{t=1}^h \frac{|\hat{y}_t - y_t|}{(|\hat{y}_t| + |y_t|)/2} \times 100\%, \end{aligned}$$

where y_t represents the observed time series, \hat{y}_t is the forecasted value, h refers to the forecast horizon, and T is the length of the in-sample (training) period. Note that the MASE metric is not defined for a single-step forecast horizon. According to standard practice, the model with the lowest error metric is regarded as the best-performing model (Hyndman & Athanasopoulos, 2018).

4.3.3. Experimental Results and Baseline Comparison

To ensure a comprehensive evaluation, the BSTS model is compared against several state-of-the-art forecasters. The implementation of BSTS is carried out in R statistical software using the *bsts* function of the *bsts* package. The optimal BSTS state specifications are listed in Table 4. The classical models ARIMA, ARFIMA, and ARNN are implemented through the *forecast* package, while the deep learning models NBeats, NHITS, DLinear, and NLinear are implemented via Python’s *darts* library. To assess the contribution of exogenous variables, all models were estimated under two distinct configurations: (i) excluding covariates, and (ii) including both the 60 statistically significant macroeconomic and financial cycle indicators along with Google Trends data. This approach facilitates a comparative evaluation of the predictive value added by incorporating these external variables into the forecasting framework.

After implementing BSTS and the baseline models, out-of-sample forecasts were generated for multiple time horizons. Tables 5 and 6 present the performance of the models based on test data, grouped into

Table 4: Presents the optimal BSTS state specifications for forecasting the US CPU index.

Horizon	State Specification
$h = 1$	Local Level, AR component, & Seasonal component
$h = 3$	Local Level, AR component, & Seasonal component
$h = 6$	Local Linear Trend, AR component, & Seasonal component
$h = 12$	Local Linear Trend
$h = 24$	Local Level, Local Linear Trend, AR component, & Seasonal component

models without covariates and models with covariates, respectively. The error metrics suggest that ARFIMA is the top-performing model for the short-term horizons, the 1-month-ahead ($h = 1$) and 3-month-ahead ($h = 3$) horizons, across both groups. In the absence of all covariates, the BSTS and ARIMA models demonstrate superior performance for both the 6-month-ahead ($h = 6$) and 12-month-ahead ($h = 12$) horizons, while the BSTS and NHiTS models produce the highest accuracy for the 24-month-ahead ($h = 24$) horizon, depending on the error metric. In contrast, BSTSX models outperform the baseline models in long-term forecasting corresponding to the 12-month-ahead and 24-month-ahead horizons, as well as the semi-long-term 6-month-ahead horizon. This outcome is anticipated since the spike-and-slab prior that BSTSX employs is highly effective at identifying and prioritizing the most relevant factors for forecasting the CPU index, thereby reducing noise and mitigating overfitting by filtering out irrelevant variables. This selective approach enhances the predictive accuracy of BSTSX, allowing it to dynamically adapt to evolving relationships within the data. This makes BSTSX highly suitable for long-term forecasting in uncertain environments. Nonetheless, when the influence of the covariates is excluded, the performance of most models improves, with BSTS and ARNN being the only exceptions. This behaviour can be explained by the absence of a variable selection method in the other models, which leads to overfitting when incorporating a large number of exogenous variables. Hence, excluding these variables mitigates the risk of overfitting, thus enhancing the accuracy of the models. However, it must be underlined that model-based forecasting, excluding covariates, is economically meaningless since the variables are relevant for capturing the underlying dynamics. Consequently, excluding them overlooks important economic factors that influence the forecast.

4.3.4. Statistical significance of the results

An evaluation of the forecasting models' performance was conducted to assess the statistical significance of differences in measurement errors by employing the model-agnostic Multiple Comparisons with the Best (MCB) procedure. MCB is a nonparametric method that ranks each of the \mathcal{M} forecasters based on their forecast accuracy across \mathcal{D} datasets (Koning, Franses, Hibon & Stekler, 2005). The model with the lowest average rank is identified as the best-performing model.

Fig. 3 depicts the ranking of the models across two groups: excluding covariates, and including the 60 statistically significant macroeconomic and financial cycle indicators along with Google Trends data. The BSTSX achieves the lowest mean rank of 2.20 for the RMSE metric across all forecast horizons, positioning it as the top-performing model, followed by BSTS (2.80), ARIMA (5.00), and ARNNX (5.60) in terms of the RMSE metric. The MCB test suggests that BSTS does not surpass the performance of BSTSX. This finding highlights the importance of incorporating covariates in forecasting the US CPU index, which is in line with observations from the tables. Despite the marginal difference in performance between BSTSX and BSTS, models that include covariates are generally preferred, as they incorporate meaningful macroeconomic and financial cycle variables. These covariates not only add valuable insights and align the forecasting process with economic theory but also make the predictions more meaningful and informative for decision-making.

Table 5: Illustrates the evaluation of the BSTS model’s performance relative to baselines across all forecast horizons without covariates. The **best** and *second-best* results are highlighted.

Horizon	Metric	ARFIMA	ARIMA	ARNN	BSTS	NBEATS	NHiTS	DLinear	NLinear
$h = 1$	MAPE	0.517	4.545	4.725	2.788	22.676	38.417	25.858	19.091
	SMAPE	0.515	4.444	4.616	2.750	20.366	32.226	22.898	17.428
	MAE	1.127	9.911	10.302	6.079	49.443	83.766	56.382	41.627
	RMSE	1.127	9.911	10.302	6.079	49.443	83.766	56.382	41.627
$h = 3$	MAPE	2.475	10.127	14.851	4.835	25.109	26.099	12.094	8.791
	SMAPE	2.424	9.631	13.768	4.720	21.324	22.964	10.932	8.160
	MAE	5.557	22.689	33.122	10.851	55.525	58.380	26.661	19.348
	MASE	0.955	3.901	5.694	1.866	9.546	10.037	4.584	3.326
	RMSE	7.334	22.906	34.013	10.932	66.629	59.811	35.585	26.287
$h = 6$	MAPE	16.229	6.553	11.970	6.314	26.716	23.478	19.156	14.447
	SMAPE	18.074	6.964	12.866	6.591	25.221	22.682	21.193	15.689
	MAE	40.169	16.982	29.592	16.142	61.027	54.649	46.868	35.648
	MASE	1.367	0.578	1.007	0.549	2.077	1.860	1.595	1.213
	RMSE	47.087	26.039	36.359	24.296	70.426	58.314	54.280	42.394
$h = 12$	MAPE	19.360	12.264	15.444	13.109	22.540	20.370	21.277	19.588
	SMAPE	22.150	12.738	18.462	13.234	22.354	21.636	22.400	20.102
	MAE	49.377	30.687	41.230	31.904	52.289	47.988	51.910	47.299
	MASE	1.415	0.880	1.182	0.915	1.499	1.376	1.488	1.356
	RMSE	61.150	43.916	65.900	41.903	60.383	55.562	64.493	58.683
$h = 24$	MAPE	36.977	24.341	22.187	20.626	23.822	22.729	25.800	22.006
	SMAPE	44.457	26.689	25.086	22.298	25.115	24.439	28.952	23.510
	MAE	90.875	59.919	56.362	51.183	56.620	54.355	63.583	53.730
	MASE	1.480	0.976	0.918	0.834	0.922	0.885	1.036	0.875
	RMSE	103.256	78.363	80.811	71.446	73.568	68.287	81.796	72.150

Table 6: Illustrates the evaluation of the BSTSX model’s performance relative to baselines across all forecast horizons using macro-financial indicators and Google Trends data. The **best** and *second-best* results are highlighted.

Horizon	Metric	ARFIMAX	ARIMAX	ARNNX	BSTSX	NBEATSX	NHiTSX	DLinearX	NLinearX
$h = 1$	MAPE	0.540	3.436	6.350	0.945	47.028	31.713	31.997	24.387
	SMAPE	0.539	3.378	6.154	0.945	38.075	27.373	27.584	21.737
	MAE	1.178	7.492	13.845	2.060	102.543	69.149	69.769	53.175
	RMSE	1.178	7.492	13.845	2.060	102.543	69.149	69.769	53.175
$h = 3$	MAPE	2.381	14.147	9.368	4.708	50.601	16.053	35.628	22.305
	SMAPE	2.329	13.582	9.317	4.598	39.630	14.401	29.489	19.806
	MAE	5.346	32.034	20.996	10.568	112.928	35.616	79.831	49.823
	MASE	0.919	5.507	3.610	1.817	19.415	6.123	13.724	8.566
	RMSE	7.384	38.779	21.123	10.655	118.719	42.559	87.526	53.186
$h = 6$	MAPE	16.299	10.896	8.186	6.029	55.015	31.979	33.733	24.987
	SMAPE	18.155	11.424	8.455	6.343	41.896	26.388	28.258	21.895
	MAE	40.330	26.575	20.230	5.572	129.318	72.532	77.783	57.627
	MASE	1.372	0.904	0.688	0.530	4.401	2.468	2.647	1.961
	RMSE	47.209	33.874	25.702	24.201	139.230	84.355	83.300	61.294
$h = 12$	MAPE	18.605	19.187	13.795	11.345	74.528	43.596	28.088	27.713
	SMAPE	21.217	21.530	15.295	12.133	52.193	34.688	25.878	25.423
	MAE	47.620	48.585	36.038	29.361	164.626	96.759	67.963	66.540
	MASE	1.365	1.393	1.033	0.842	4.719	2.774	1.948	1.907
	RMSE	59.830	66.708	59.739	44.153	177.004	107.107	87.748	82.833
$h = 24$	MAPE	36.951	27.282	24.502	18.194	32.408	34.603	36.579	29.985
	SMAPE	44.414	32.126	26.489	19.182	32.406	39.809	42.008	33.742
	MAE	90.807	69.591	59.253	44.670	81.390	89.026	89.146	77.392
	MASE	1.479	1.134	0.965	0.728	1.326	1.450	1.452	1.261
	RMSE	103.194	91.093	77.387	66.440	109.319	116.036	112.517	102.789

The upper limit of the critical distance for BSTSX, represented by the gray-shaded region in Fig. 3, serves as a benchmark for comparison. Models such as NLinearX, NHiTSX, DLinearX, and NBEATSX have critical intervals much higher than this benchmark, indicating that their performance is substantially inferior to that of BSTSX. Notably, the inclusion of covariates improves the performance of BSTS and ARNN, whereas the performance of the other models generally deteriorates, which is consistent with results reported in subsection 4.3.3. This suggests that BSTS and ARNN are better equipped to handle high-dimensional covariates by effectively extracting relevant information that explains more of the variability in the CPU series. This, in turn, enhances their predictive accuracy. In contrast, the remaining statistical and deep learning models appear to struggle with the increased complexity and noise introduced by the large number of covariates, leading to overfitting and a decline in performance. Overall, this analysis highlights the statistical differences in model behavior and further supports the superior performance of the BSTSX model across different forecasting horizons.

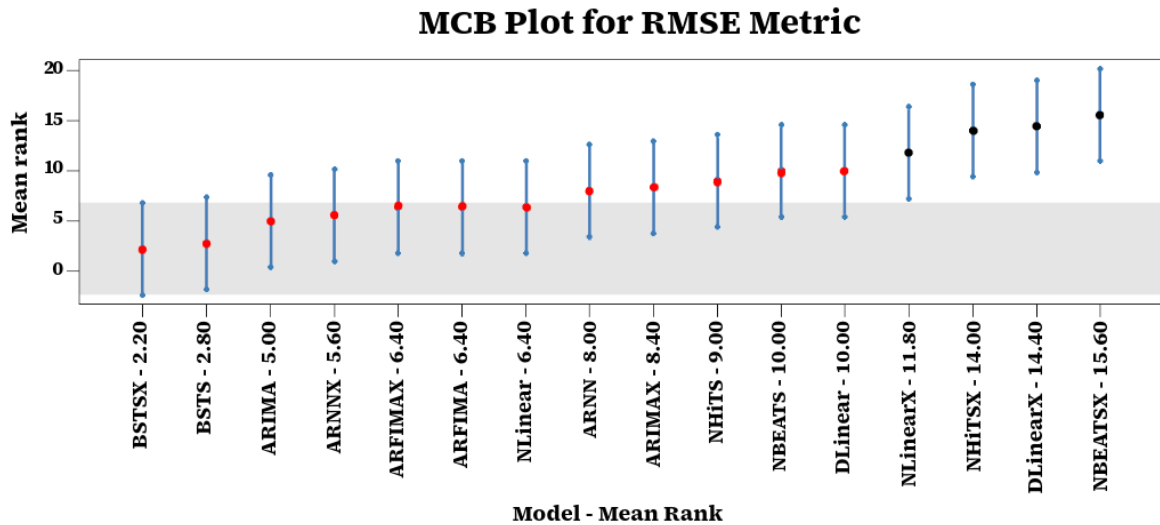


Figure 3: Portrays the MCB plot for the models across the two categories. BSTSX-2.20, for instance, signifies that the average ranking of the BSTSX model, according to the RMSE metric, is 2.20. This same interpretation holds for other models.

In addition to the MCB test, we employ the Murphy diagram approach to evaluate the robustness and forecastability of the BSTSX model. Unlike the MCB method, which focuses on ranking models based on their average forecast accuracy, the Murphy diagram evaluates whether a forecasting model consistently outperforms alternative models across a diverse set of loss functions (Ehm, Gneiting, Jordan & Krüger, 2016; Ziegel, Krüger, Jordan & Fasciati, 2017). This diagram is constructed by calculating the model’s performance scores under multiple scoring functions, enabling a detailed comparison of empirical forecast accuracy. The Murphy diagram is formed by evaluating the following scoring function:

$$\tilde{s}(\hat{y}_t, y_t) = \begin{cases} |y_t - \theta|, & \min(\hat{y}_t, y_t) \leq \theta < \max(\hat{y}_t, y_t) \\ 0, & \text{otherwise,} \end{cases} \quad (2)$$

where y_t denotes the observed value at time t , \hat{y}_t is the forecast generated by the model, and the parameter $\theta \in \mathbb{R}$ determines the shape of the loss function. The parameter θ acts as a threshold sliding between the forecast and the observation, enabling the scoring function to highlight different aspects of forecast errors. Specifically, lower values of θ increase the penalty for underestimations, while higher values place greater weight on overestimations. To assess the relative performance of competing forecasting models, the average

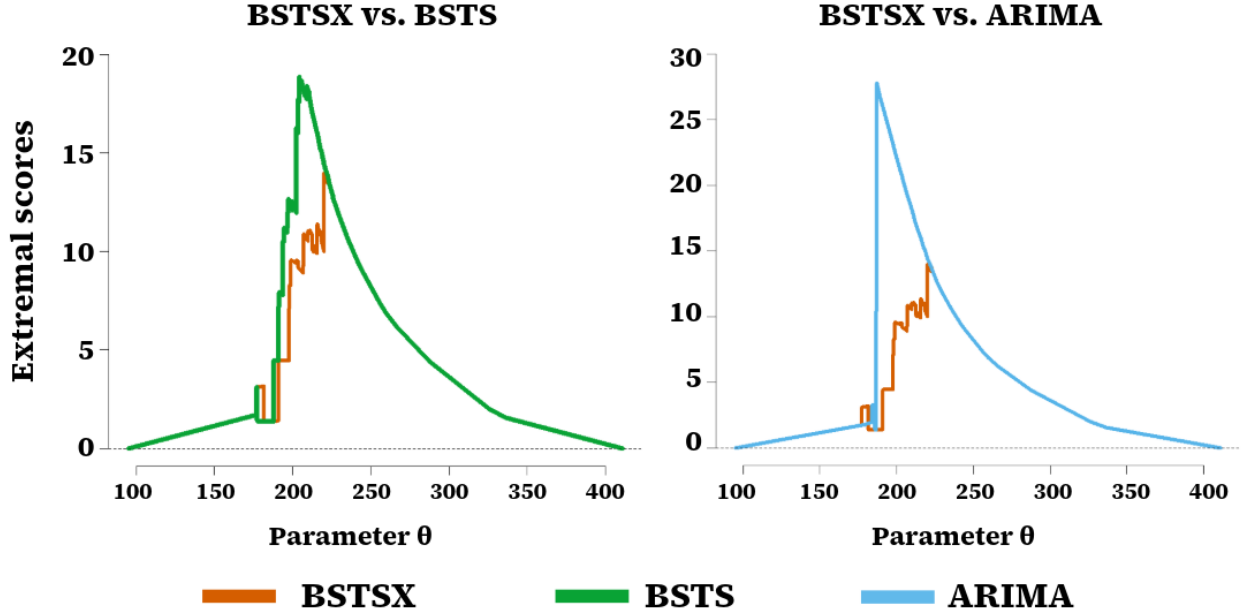


Figure 4: Displays the Murphy diagrams of BSTSX with baselines (BSTS (left) and ARIMA (right)) for the 24-month ahead CPU index forecasts. The parameter θ represents the shape parameter as defined in Eqn. (2). Lower scores indicate better performance.

score for model j over a forecast horizon of length h is computed as:

$$\mathcal{S}_j(\theta) = \frac{1}{h} \sum_{t=1}^h \tilde{s}(\hat{y}_{t,j}, y_t),$$

where $\hat{y}_{t,j}$ is the forecast from model j at time t and h is the forecast horizon. Plotting the average scores $\mathcal{S}_j(\theta)$ across a range of values of θ yields the Murphy diagram. Consequently, the Murphy diagram serves as a flexible and insightful tool to identify models that consistently outperform others across diverse scoring functions. To assess the empirical performance of the BSTSX model relative to the benchmarks, we employed the `murphydiagram` package in **R** to construct Murphy diagrams. This visualization facilitates detailed pairwise comparisons by evaluating the BSTSX model against BSTS and ARIMA, the top-performing models in the RMSE-based MCB test. Fig. 4 displays the Murphy diagrams comparing BSTSX with the baseline models over a 24-month-ahead forecasting horizon. Lower extremal scores indicate superior forecasting performance. To complement this comparison, Fig. 5 illustrates the Murphy difference diagram, which presents the difference in extremal scores between models along with 95% confidence intervals, where negative values indicate that BSTSX outperforms the benchmark model at a given value θ . Thus, offering additional evidence of BSTSX's forecasting advantage. Figs. 4 and 5 demonstrate that BSTSX consistently outperforms both BSTS and ARIMA across various values of θ , with a marked advantage particularly evident in the lower to mid θ range. This supports the findings from the RMSE-based MCB test and highlights the value of incorporating macroeconomic and financial cycle indicators, along with Google Trends data, into the forecasting model. However, as θ exceeds approximately 225, the performance advantage of BSTSX diminishes, suggesting that under higher overprediction penalties, the improvement becomes less pronounced. Overall, this evaluation highlights the robustness of BSTSX as a forecasting method. By combining the insights from both MCB tests and Murphy diagrams, we provide strong and comprehensive evidence of the model's forecasting superiority, positioning it as a reliable and effective forecasting framework.

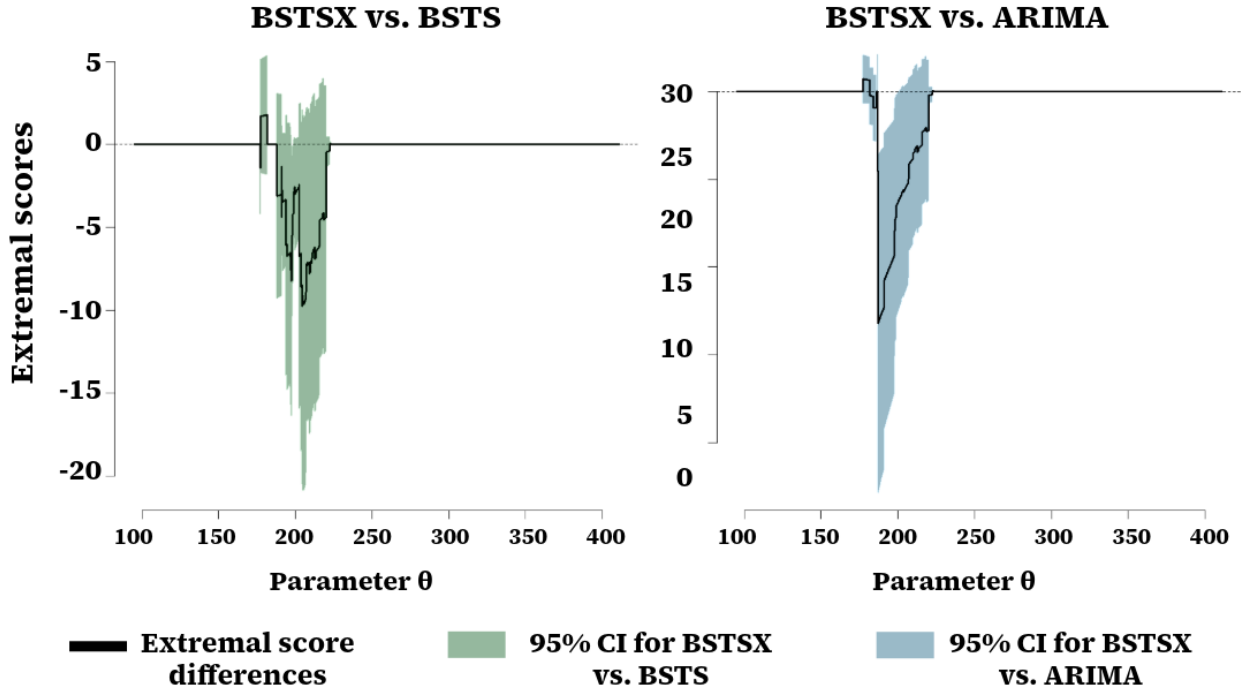


Figure 5: Displays the Murphy difference diagrams of BSTSX with baselines (BSTS (left) and ARIMA (right)) for the 24-month ahead CPU index forecasts. The parameter θ represents the shape parameter as defined in Eqn. (2). A negative score difference indicates that BSTSX outperforms its competitor.

5. Important Features and Impulse Response Analysis

5.1. Economic Interpretation of Feature Importance Plot

In subsection 4.3.3, we noted the ability of covariates to forecast the US CPU index. We also noted the superior performance of the BSTS model in comparison to other machine learning and deep learning models. For interpretability purposes, we focus on the macroeconomic and cycle financial variables and omit the Google Trends data. However, their significance is evident from Fig. 2, where the time series of several climate-related search terms closely mirror the evolution of the US CPU index, confirming their complementary value in capturing public sentiment around climate policy uncertainty. In order to explore the ability of the macroeconomic and financial cycle variables in forecasting the US CPU index, we portray the feature importance plot generated by the BSTS model over the 24-month-ahead forecast horizon, referring to the most vital variables contributing to forecasting the CPU index. The inclusion of the feature importance plot significantly enhances the policy relevance and interpretability of the BSTS model in this study. This analysis provides economic reasons behind the BSTS model’s forecasting power. Fig. 6 highlights the variables with the highest inclusion probabilities, such as `mortg_inc` (Mortgage/Income ratio), `BCI` (Business Confidence Index), `CAPE` (Cyclically Adjusted Price/Rent ratio), and housing permits. These variables represent broad sectors of the overall economy, such as the financial market sector, the housing sector, the labor market, and economic sentiment that policymakers should take into consideration while framing climate strategies. Beyond forecasting accuracy, the feature importance plot analysis highlights how macroeconomic and financial cycle variables give early signs of uncertainty related to climate policies. This analysis will not only complement the impulse response analysis, in Section 5.2, but also give a clear understanding of the structural macroeconomic and financial market forces that drive CPU. Hence, it positions the

BSTS framework as both a forecasting and an explanatory tool for climate-policy-related decision-making.

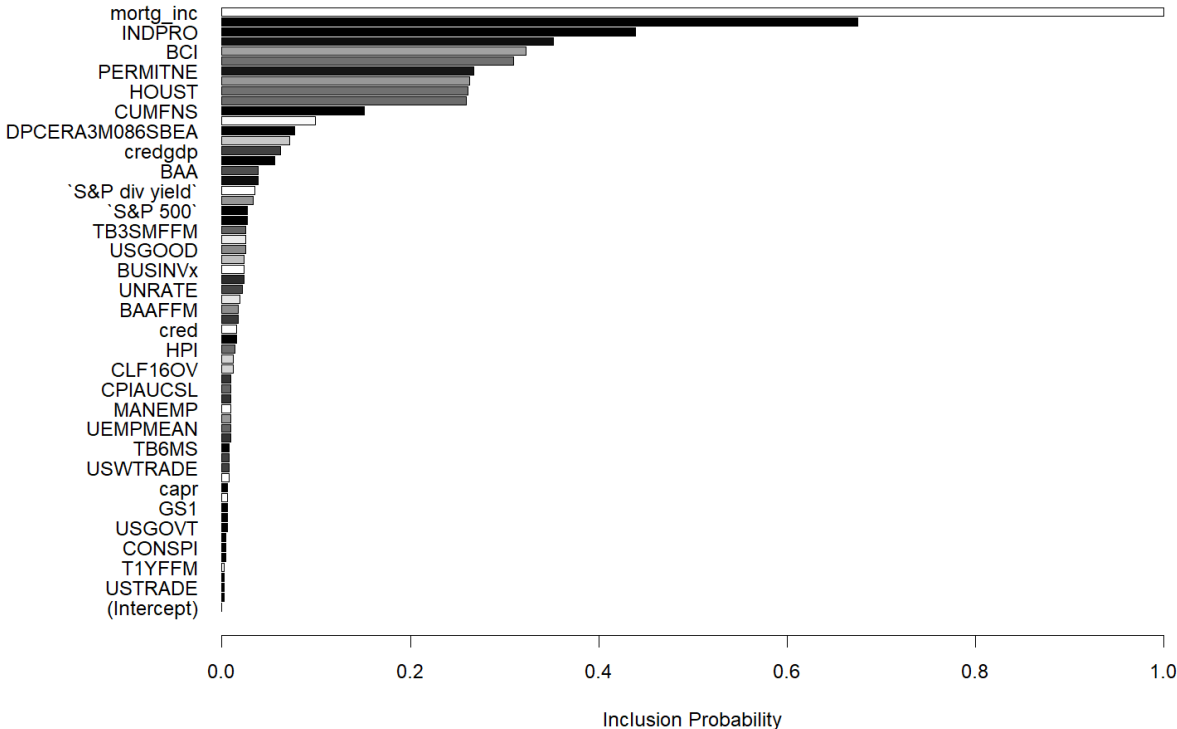


Figure 6: Depicts the inclusion probabilities of variables selected by the BSTS model over a 24-month-ahead forecast horizon. The plot reflects the relative importance of each variable in contributing to the model’s predictive accuracy, with higher probabilities indicating greater explanatory relevance.

From the feature importance plot in Fig. 6, we consider the first ten variables with the highest probabilities of inclusion in the BSTS model. These ten variables are intuitively and intrinsically linked to significant macroeconomic and financial factors that affect CPU. At the top of the feature importance list is the *mortg_inc*, reflecting the amount of loans related to the financial stress of individual households due to home loan mortgages. The financial stress increases when the central banks increase the interest rates. High levels of home loans and their interest rates reduce the disposable income of the household, making it more challenging for the public to accept climate policy changes or regulations that could increase living costs. This public opposition can put pressure on policymakers to soften or postpone such environmental initiatives. The industrial production index (*INDPRO*) monitors real economic output across major industrial production sectors of the US and is also playing a very important role due to its direct correlation with energy consumption and emissions. The fluctuations in the industrial sector output may discourage the adoption of new climate regulations by firms, which will make it difficult for policymakers to strike a delicate balance between economic growth and maintaining environmental sustainability. Such a scenario impacts the credibility and timing of climate action initiatives. *BCI* reflects the corporate forward-looking expectations about the economy and their readiness for additional investment. This is very important in assessing whether businesses are inclined to commit additional investments to comply with green regulations. A strong *BCI* signals optimism about the economic future, potentially encouraging businesses to support and adopt environmental policies. Conversely, a weak *BCI* may lead to reluctance in embracing such regulations during periods of economic uncertainty. Both *BCI* and *INDPRO* are key indicators closely tied to business sector performance. *INDPRO* reflects the current state of the industrial sector, whereas *BCI* reflects the future economic outlook of businesses, emphasizing expectations about the future. These results suggest that CPU is dependent on the state of the underlying economy (Zhang & Chiu, 2020). Housing metrics

such as New Private Housing Permits in the Northeastern part of the US (PERMITNE) and total housing starts (HOUST) reflect the housing sector dynamics of the economy. It portrays the real estate development conditions that may help governments to plan and implement long-term climate policies more readily. High values of PERMITNE and HOUST reflect the vitality of the construction sector, thus reflecting the robustness of the economy. This is often linked with optimism in the economy, thereby enabling the government to implement long-term climate goals, as people will be more adaptable to climate change policies owing to their economic stability. At this stage, people will also be flexible in adopting climate-friendly installations in their new homes. However, low levels of housing permits and new home construction may indicate economic stagnation, potentially causing delays in environmental policy implementation aimed at protecting the real estate sector, a key driver of business cycles. A stricter environmental regulation can make the housing and real estate sector vulnerable (Cho, Yang & Jang, 2024). The impact of these regulations will be worse if the housing sector is already grappling with the weak broader economy. Manufacturing capacity utilization (CUMFNS) measures the degree to which the economy is utilizing its existing productive capacity. High capacity utilization can create resource constraints and trigger inflationary pressures, potentially prompting interest rate tightening. Conversely, low capacity utilization may encourage interest rate cuts intended to support economic recovery. A lower interest rate scenario helps businesses to invest heavily in renewable energy-related infrastructure and adopt clean energy policies. The transition towards alternative sources of energy requires heavy investment. A low interest rate reduces the cost that will be incurred to make the necessary transition to adopt the environmentally friendly infrastructure by businesses. Closely related to these investment dynamics is consumer spending, which plays a critical role in shaping economic activity and environmental policy support. The variable representing consumer spending, real personal consumption expenditures (DPCERA3M086SBEA), is very important as the US is a consumption-based economy. A robust consumption growth signifies a period of economic prosperity, which will prompt the government to take action on climate change and implement stricter policies. A fall in the demand side of the economy often results in climate policy initiatives being delayed. This depicts the dependency of the climate policy initiatives on the economic uncertainty (Zhang & Razzaq, 2022). The credit-to-GDP ratio (credgdp) reflects the systemic leverage within the economy; a high ratio signals elevated credit levels relative to GDP, increasing financial vulnerability and potentially discouraging policymakers from implementing significant changes that might destabilize markets. During periods of high credit-to-GDP ratio, central banks push for stricter macro-prudential policies that restrict credit growth in the economy. This lowered credit growth may delay the adoption of climate policies by businesses. Additionally, the S&P 500 dividend yield and the Moody's Seasoned Baa Corporate Bond Yield (BAA) reflect capital expenditure, credit risk, and market sentiment. Particularly in capital-intensive sectors and regulated industries, increases in bond yields and high dividend yields are associated with investor caution and increased sensitivity to climate policy risk. This risk-aversion behaviour among investors can delay the adoption of climate-friendly policies. The above-mentioned ten factors cover broad sectors of the economy, public sentiment, sectoral risk exposure to policy, and macro-financial stability (Annicchiarico et al., 2022, Giovanardi & Kaldorf, 2024). All of these factors have been found to have a significant impact on the CPU in the US.

5.2. Impulse Response Analysis

One of the issues of the feature importance plot obtained from the BSTS model, depicted in Fig. 6, is that the variables identified to forecast the CPU index are statistically relevant, but fail to capture the dimension of the temporal evolution of these relationships. Hence, to further enhance the economic intuition and significance of the results, this subsection examines the responses of the CPU to shocks originating from key macroeconomic and financial cycle variables. The impulse response analysis is conducted using the local projections method of Jordà, 2005, which is well-suited in this context due to its resilience to model misspecification and its flexibility in estimating dynamic effects without imposing restrictive assumptions often associated with vector autoregression (VAR) models. Given the structural uncertainty and high dimensionality associated with the determinants of the CPU index, the local projection approach offers a

transparent framework for examining how shocks, such as an increase in unemployment or shifts in credit markets, impact CPU across various time horizons. This approach is particularly beneficial in climate policy-related research, where grasping the timing, volatility, and persistence of policy uncertainty is essential for crafting adaptive and forward-thinking strategies. Therefore, the impulse response analysis through local projections enhances the BSTS findings by providing deeper insights into the dynamic transmission processes between macroeconomic and financial cycle factors and CPU.

The impulse response analysis focuses on sixteen variables: Business Confidence Index (BCI), Composite Leading Indicator (CLI), Real S&P500 Index Growth (SP500), Cyclically Adjusted Price/Earnings ratio (CAP/Earnings), Real Credit Growth (CRED), Credit/GDP ratio (CRED/GDP), House Price Index (HPI), Price/Rent ratio (CAP/Rent), Household Real Mortgage Debt Growth (Mortgage), Household Mortgage/Income ratio (Mortgage/Income), Private Residential Fixed Investment/GDP ratio (PRFI/GDP), Personal Interest Payments/Income ratio (PIP/Income), Unemployment Rate (UNRATE), Total Housing Starts (HOUST), Real Personal Consumption Expenditures (DPCERA3M086SBEA), and New Private Housing Permits in the Northeastern part of the US (PERMITNE). These variables have statistically significant causal effects on the CPU index. In addition, these included variables represent the widest spectrum of the overall aggregate macroeconomy, covering major sectors, such as labor, credit, housing, consumption, and financial markets, to provide exploratory insights into how broader macroeconomic conditions influence the CPU index.

This analysis employs the local projections methodology on monthly data spanning April 1987 through June 2023 to identify the dynamic impact of financial and macroeconomic disturbances on the CPU index. The estimation of Impulse Response Functions (IRFs) follows the local projections methodology originally developed by [Jordà, 2005](#), and computationally implemented by the `lpirfs` package in **R** [Adämmer, 2019](#). This approach fundamentally differs from the VAR method by employing direct sequential regressions on future realizations of the dependent variable, thereby preventing the necessity to specify and invert a complete multivariate dynamic system ([Jordà, 2005](#)). The local projections framework provides three key methodological advantages: enhanced robustness to model misspecification, direct analytical inference, and capacity to flexibly model nonlinear dynamics and accommodate varied data structures without imposing strong a priori restrictions on the data-generating process ([Jordà, 2005](#); [Adämmer, 2019](#)). This study employs linear local projections estimated via the `lp-lin` function with the following specifications: a maximum lag length of 12 months determined by the Bayesian Information Criterion (`max-lags = 12`), a linear time trend (`trend = 1`), shocks standardized to one standard deviation (`shock-type = 0`), and 95% confidence intervals computed using heteroskedasticity and autocorrelation-robust Newey-West ([Newey & West, 1987](#)) standard errors (`confint = 1.96`, `use-nw = TRUE`). The analysis estimates impulse response functions across a 24-month-ahead horizon (`hor = 24`). The IRFs presented in [Fig. 7](#) reveal the dynamic response patterns of the CPU index to these shocks across a 24-month-ahead horizon.

In this study, the CPU index measures the degree of uncertainty in climate-related policy, with higher values indicating greater uncertainty. This is essential for interpreting the impulse response results: a positive impulse response signifies an increase in CPU, while a negative response denotes a reduction in uncertainty. [Fig. 7](#) illustrates the dynamic responses of the CPU index to shocks originating from macroeconomic and financial cycle variables. The impulse response analysis shows that the variables have economically meaningful and statistically significant effects on the CPU Index, either positively or negatively. Among the variables that have positive influences, CAP/Earnings stands out with a steadily increasing positive effect over the 24-month-ahead horizon, indicating a persistent and robust relationship where overvaluation in equity markets increases the CPU. A positive relation between CAP/Earnings and CPU suggests that when the markets have high valuations, any regulation change, including climate-related policies such as an increase in environmental taxes or upgradation of production facilities, can increase the companies' costs and reduce their profitability. Reduced earnings in the period of overvalued financial markets lead to a sharp market correction. Hence, during market overvaluation, the investors can be very sensitive to changes in climate-

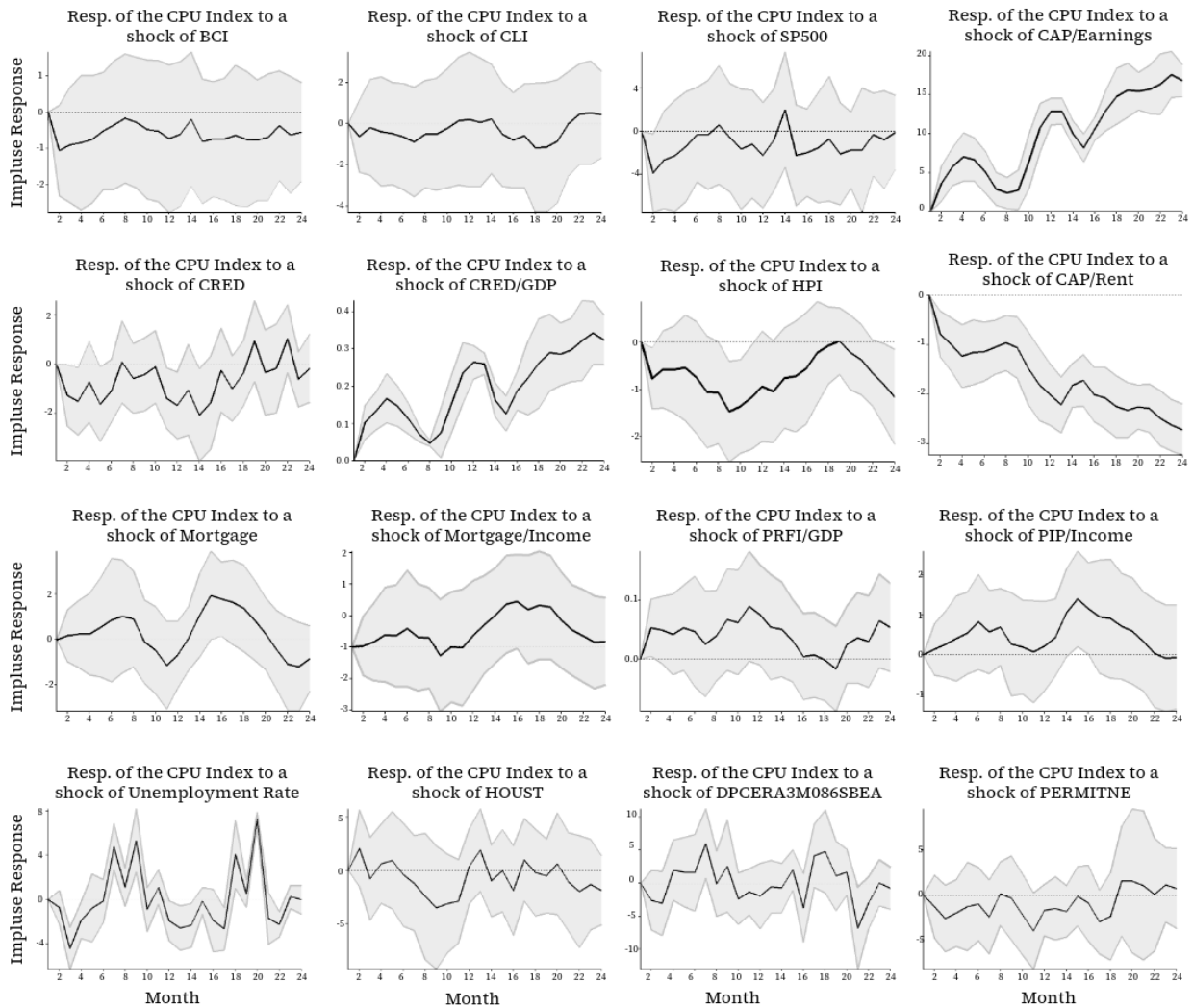


Figure 7: Illustrates the impulse response functions generated via the local projections method, quantifying the CPU index’s dynamic reactions to shocks in macroeconomic and financial cycle variables. The reaction is represented by the solid black line, and the 95% confidence intervals are represented by the gray shaded regions. The dashed black line displays the zero line. The sample period runs from April 1987 to June 2023.

related regulatory policies, thereby increasing the perceived uncertainty. Similarly, CRED/GDP shows a robust positive effect and stands out with a steadily increasing positive effect over the 24-month-ahead horizon. CRED/GDP reflects systemic leverage; an elevated level of credit relative to GDP heightens financial vulnerability, which may discourage policymakers from implementing substantial policy changes that could destabilize corporate financial situations (Annicchiarico et al., 2022). Adoption and compliance with any new climate regulation require substantial business investment. Central banks can introduce stricter macro-prudential policies to restrict credit and systemic vulnerability in the environment of excessive credit growth relative to the GDP. In this case, a stricter credit policy can discourage the business from making new investments for compliance with new climate regulations, thereby increasing the uncertainty related to climate policies. The impulse of response of the CPU to PIP/Income also exhibits a positive response. This response is statistically significant between the 14th- and 16th-month-ahead horizons. This positive relationship implies that when households face higher interest payments relative to their income to service

debt, they become more sensitive to regulatory changes, including those related to climate policy. This reflects a tension between the increased financial vulnerability of individual households and the perceived cost of implementing climate policy regulations. Further adding to the evidence of CPU being dependent on the cyclical macroeconomic variables is its positive impulse response relationship with the variable unemployment rate. When the unemployment rate increases, the focus of the people shifts from environmental concerns to basic survival needs. This again makes the households reluctant to comply with any new environmental policies, thereby making the introduction and implementation of any changes to climate policy regulation very difficult and politically sensitive. This observation is in line with the findings of (Le, 2025), who observed that positive carbon policy shocks lead to a fall in the aggregate output in the economy by 0.7% and it will lead to an increase in inflation by 0.3%. During periods of elevated unemployment rates, any stricter climate regulation will deepen the recession and further increase unemployment in the economy. Lastly, we observe a positive impulse response relationship of CPU with the variable PRFI/GDP. A greater PRFI/GDP indicates a rise in residential construction, which may lead to increased environmental consequences such as elevated energy consumption, land development, and construction-related emissions. This may drive policymakers to propose stricter climate regulations to alleviate the threats to environmental or climatic degradation. The policies may include stricter emission controls, increased taxes, or changes in the building standards. This expectation of any forthcoming rigorous and stringent policies can increase uncertainty surrounding climate policy, regarding their timing and intensity, thereby positively influencing the CPU Index. Though the effect is for an initial short period of 2 months (Cho et al., 2024).

Now we shift our focus to the variables that exert a negative and statistically significant influence on the CPU Index. The CAP/Rent depicts an intensely negative and consistent impact throughout 24 24-month horizon. The economic intuition behind this effect's sustained nature is that an increase in property prices relative to rental income reflects an increase in the net worth of the homeowners and creates a wealth effect. An increase in the real estate asset price can be linked with reduced uncertainty and increased investor confidence, making them more optimistic about the future economic outlook. Increased optimism about the future economic outlook, coupled with increased wealth, makes individuals and businesses more adaptive to climate change policies. Similarly, HPI demonstrates a negative and statistically significant response. The negative response suggests that increasing house prices signal economic stability and rising housing demand. This improved economic stability may reduce CPU as people are expected to have a higher disposable income to comply with new environmental or climate regulations. Hence, the policymakers have lower resistance from people and lower political pressure to alter existing environmental policies (Obani & Gupta, 2016, Bumann, 2021). The variable CRED shows a negative but short-lived effect on the CPU. The negative effect of CRED on the CPU is significant for only the first 2 months. The initial negative response can be attributed to the fact that business cycles alternate between economic recovery and recession. When the economy enters the recovery phase following a recession or stagnation, an initial wave of credit growth typically emerges, driven by rising investment and employment opportunities at the start of the new cycle. This period is often marked by robust corporate profits and growing household incomes, thereby creating a favorable environment for policymakers to simultaneously introduce and implement ambitious climate-related policies. However, when credit growth exceeds the growth rate of economic output, the resulting increase in credit can heighten climate-related uncertainties, as previously discussed in the case of CRED/GDP. Regarding the S&P 500, it demonstrates a negative and statistically significant impact on the US CPU during the first 2 months following a positive shock. Rising stock prices in equity markets lead to increased wealth in the hands of investors. The positive wealth effect creates positive sentiment about the economy among investors. The forward-looking optimism enhances the commitment of households and businesses towards adherence to any new changes in environmental and climate change regulations. S&P 500 acts as a sentiment barometer for the aggregate macroeconomy, which influences the perceived viability of climate-friendly and environmental investments. Such enhanced commitment and positive economic outlook give an opportunity to policymakers to pursue and implement new climate change policies. The opposite scenario occurs during a recession-driven bear market when negative forward-looking behaviour makes it difficult for policymakers to implement stricter climate policies (Khan, Metaxoglou, Knittel & Papineau,

2019; Amin & Dogan, 2021).

The results mentioned above signify the dynamic interlinkages between the US CPU and business as well as financial cycle variables. Also, we can observe that any positive shocks to macro-financial variables, indicating a robust economic scenario, yield a reduction in the CPU. Similarly, any positive shocks to macro-financial variables, indicating a weak economic scenario, yield an increase in the CPU. This confirms the dependence of climate-related policy uncertainty on the underlying condition of the state of the economy.

6. Policy Implication

This study unravels a complex and nuanced relationship between the macroeconomic-financial variables and the US's CPU. The results of this study highlight the pivotal role of prevailing macroeconomic conditions and financial vulnerabilities in forecasting the uncertainties related to climate policies. This study applied a wide range of classical, machine learning, and deep learning methods to unravel the importance of macro-financial variables and Google Trends data in forecasting the US CPU index. The BSTS model demonstrated the highest forecasting accuracy for the CPU index compared to other statistical and deep learning models, such as ARIMA, ARFIMA, ARNN, NBeats, NHiTS, DLinear, and NLinear. This superior performance can be attributed to its robust variable selection mechanism via the spike-and-slab prior. This prior enables the model to incorporate a broad set of exogenous variables, including macroeconomic indicators, financial cycle measures, and Google Trends data, thereby enhancing its forecasting capability. The results of the proposed BSTS model have important implications for policymakers endeavoring to strike a balance between macro-financial stability and environmental sustainability.

A key insight from this study is the critical influence of macroeconomic and financial cycle variables on CPU. Variables such as the Cyclically Adjusted Price/Earnings (CAPE) ratio, Business Confidence Index (BCI), Composite Leading Indicator (CLI), Household Mortgage-to-Income (Mortgage/Income) ratio, and New Private Housing Permits in the Northeastern part of the US (PERMITNE) emerged as significant predictors of CPU. An increase in the CAPE ratio indicates the potential overvaluation in asset prices that often coincides with inflationary pressures. The central banks in this situation increase interest rates to control inflation and reduce asset price bubbles, which deters the firms and the individual households from investing in new green technologies, leading to an increase in the uncertainty of climate policy. Similarly, the Mortgage/Income ratio reflects household financial stress, which can lead to public resistance against climate policies perceived as increasing living costs, further complicating policy implementation (Khan et al., 2019; Amin & Dogan, 2021). The BCI and CLI give forward-looking insights into the economic situations of firms and individuals, respectively. Higher values of these two indicators signify the readiness of households and corporate confidence to invest in new technologies or pay additional taxes to comply with new environmental regulations, thereby reducing CPU. Conversely, a weak BCI or CLI signals economic downturns, often shifting governmental focus toward short-term economic recovery, thus relegating climate policies to secondary priority (Sultanuzzaman et al., 2024; Gaies, 2025). This cyclical behaviour aligns with prior literature, which notes that economic recessions tend to undermine climate policy commitments as governments prioritize fiscal stimulus and job creation (Ide, 2020). PERMITNE serves as a barometer of economic vitality. High permit activity indicates a robust real estate development in the economy. This creates a favourable environment for policymakers to implement stricter climate policies that households will comply with, owing to higher economic growth. However, a low real estate activity signals economic stagnation, often leading to delays in environmental regulations to protect the real estate sector. Hence, the feature importance generated by the BSTS model via the spike-and-slab prior is not only statistically robust but also yields sound economic reasoning.

To give further robustness in our study, we conducted impulse response analysis with the help of the

Local Projection method. The impulse response analysis further enriches our findings by giving the dynamic responses of the CPU to shocks in macroeconomic and financial variables. For example, positive shocks of the CAPE ratio and CRED/GDP (credit-to-GDP) ratio increase the CPU, reflecting heightened investor sensitivity to regulatory changes during periods of market overvaluation or excessive leverage. Conversely, shocks of variables such as the HPI (House Price Index) and S&P 500 Index Growth reduced CPU, as rising asset prices signal economic stability and foster optimism, making households and businesses more receptive to climate policies. These results give support to our hypothesis that CPU is highly sensitive to the underlying state of the economy, with strong economic conditions facilitating policy stability and weak conditions exacerbating uncertainty.

The inclusion of Google Trends data as a proxy for public sentiment also proved valuable, particularly for long-term forecasting. We considered search terms such as “climate policy” and “climate risk” to capture the variations in the CPU index. They indicate the public interest and awareness in issues related to climate change and regulations, thereby serving as early indicators of policy uncertainty. The results of our study underscore the importance of integrating non-traditional data sources into economic forecasting models to capture societal dynamics that influence policy environments. Despite the BSTS model’s superior performance, the study reveals challenges in short-term forecasting, where ARFIMA outperformed BSTS in the short-term forecasting horizons (1- and 3-month-ahead). This may be due to the statistical models’ ability to leverage the long-range dependencies and autocorrelation structures in the CPU series more effectively in the short-term horizons. However, for longer horizons (6-, 12-, and 24-month-ahead), the BSTS model’s ability to dynamically select relevant predictors and mitigate overfitting through the spike-and-slab prior made it the preferred choice. This adaptability is especially valuable when modeling phenomena driven by long-term trends and structural shifts.

The findings in this study have practical implications for both policymakers and industry stakeholders. By identifying key macroeconomic and financial sector drivers of CPU, such as housing market activity, credit-to-GDP ratio, unemployment rate, and financial market valuations, this study will help policymakers to be better equipped to anticipate periods of heightened uncertainty related to climate policies and accordingly tailor their strategies. For example, during a recession, the government and policymakers can prioritize and propose green stimulus packages that align economic recovery with climate goals. Previously, in 2020, the European Union’s and South Korea’s Green deals served the dual objective of economic recovery from the pandemic and promoting clean energy policies. These relief packages allocated funds to green projects and gave their commitment to a decarbonized recovery from the COVID-19 recession. Similarly, the US, in its fiscal stimulus during the Great Recession of 2008, allocated 90 billion US Dollars to promote clean and efficient energy. Such policies mitigate the trade-off between short-term macroeconomic stability and long-term environmental sustainability. Similarly, industries sensitive to policy uncertainty, such as renewable energy and manufacturing, can use these insights to time their investments more effectively, avoiding periods of high CPU that could jeopardize returns.

This study only focuses on US data. This US-centric focus inhibits the generalizability of the findings in this study to developing nations having different economic structures and environmental regulatory frameworks. While the policy insights drawn from the US context are valuable, it is important to acknowledge the geographic limitations of this analysis. Future studies can take into consideration global macroeconomic variables or regional climate policy indices to provide a more comprehensive view of the dynamics of the uncertainties related to climate policies and environmental regulations. This study has established the BSTS model as a powerful tool for forecasting CPU, given its ability to integrate a high-dimensional set of exogenous variables, including a diverse range of macroeconomic, financial cycle, and sentiment-based variables. The results highlighted the cyclical nature of CPU, with robust economic growth fostering policy stability and recessions exacerbating its uncertainty. These observations provide a strong foundation for more informed policymaking and strategic planning in the pursuit of attaining a triple objective of economic growth, a clean environment, and mitigating the issue of climate sustainability.

7. Conclusion

The purpose of the study was to investigate the CPU series and assess the influence of the US macroeconomic and financial cycle variables, together with Google Trends data, for forecasting the CPU index. The BSTS model was selected to forecast the CPU index due to its adaptability under uncertain conditions and its robust variable selection mechanism, the spike-and-slab prior, that identifies and incorporates the most relevant variables, ensuring improved accuracy in capturing the complex dynamics of the CPU series. This study determined that the CPU series is significantly influenced by both the US macroeconomic and financial cycle variables and Google Trends data. The findings highlight the BSTS model's effectiveness in producing superior CPU index forecasts in comparison to alternative statistical and deep learning approaches.

One limitation of this study lies in the structural shifts observed in the CPU index over time. As illustrated in Fig. 1, the CPU index follows three distinct phases marked by significant shifts in magnitude: the period before 2000, the wave of rapid technological advancement during the early 2000s to the late 2010s, and the current phase marked by the rise of artificial intelligence developments. These structural changes may affect the stability and consistency of forecast accuracy. To address the shifting behaviour of the CPU index across distinct phases, future research could apply regime-switching models or explore nonlinear Bayesian methods to capture structural breaks and nonlinear dynamics more effectively. Additionally, conducting phase-specific analyses might provide deeper insights into the drivers of CPU in each era. Moreover, expanding the dataset to include global macroeconomic and technological indicators may improve the model's ability to adapt to evolving economic environments. Furthermore, integrating machine learning techniques that handle nonstationarity and structural shifts, such as recurrent neural networks, could further enhance forecast accuracy. Lastly, examining the role of green financing and renewable energy adoption at the sector level could provide policymakers with more targeted insights to support a sustainable economic transition.

Code and Data Availability

The US Climate Policy Uncertainty (CPU) index series used in this study was obtained from the Economic Policy Uncertainty website: https://www.policyuncertainty.com/climate_uncertainty.html. The code used to perform the analyses and generate the results is available at: https://github.com/Donia-212/Climate_Policy_Uncertainty_Forecasting/tree/main. The repository contains all datasets and code necessary to reproduce the findings presented in this paper.

Acknowledgement

The authors want to thank Madhurima Panja of IIIT Bangalore, India, for the discussion and help with the graphics presented in this manuscript.

References

- Adämmer, P. (2019). Ipirfs: An r package to estimate impulse response functions by local projections, .
- Adebayo, T. S., Kartal, M. T., Ağa, M., & Al-Faryan, M. A. S. (2023). Role of country risks and renewable energy consumption on environmental quality: Evidence from mint countries. *Journal of Environmental Management*, 327, 116884.

- Akan, T. (2024). The impact of monetary policy on climate change through the mediation of sectoral renewable energy consumption. *Energy Policy*, *192*, 114244.
- Amin, A., & Dogan, E. (2021). The role of economic policy uncertainty in the energy-environment nexus for china: evidence from the novel dynamic simulations method. *Journal of Environmental Management*, *292*, 112865.
- Annicchiarico, B., Carattini, S., Fischer, C., & Heutel, G. (2022). Business cycles and environmental policy: A primer. *Environmental and energy policy and the economy*, *3*, 221–253.
- Arouri, M., Gomes, M., & Pijourlet, G. (2025). Does climate policy uncertainty shape the response of stock markets to oil price changes? evidence from gcc stock markets. *Journal of Environmental Management*, *375*, 124229.
- Balsalobre-Lorente, D., Driha, O. M., Halkos, G., & Mishra, S. (2022). Influence of growth and urbanization on co2 emissions: The moderating effect of foreign direct investment on energy use in brics. *Sustainable Development*, *30*, 227–240.
- Bauer, M. D., Offner, E. A., & Rudebusch, G. D. (2023). *The effect of US climate policy on financial markets: An event study of the Inflation Reduction Act*. Technical Report CESifo Working Paper.
- Berestycki, C., Carattini, S., Dechezleprêtre, A., & Kruse, T. (2022). *Measuring and assessing the effects of climate policy uncertainty*. Technical Report 1724 OECD Economics Department Working Papers.
- Box, G. E., Jenkins, G. M., Reinsel, G. C., & Ljung, G. M. (2015). *Time Series Analysis: Forecasting and Control*. John Wiley & Sons.
- Box, G. E. P., & Pierce, D. A. (1970). Distribution of residual autocorrelations in autoregressive-integrated moving average time series models. *Journal of the American Statistical Association*, *65*, 1509–1526.
- Brodersen, K. H., Gallusser, F., Koehler, J., Remy, N., & Scott, S. L. (2015). Inferring causal impact using bayesian structural time-series models, .
- Bumann, S. (2021). What are the determinants of public support for climate policies? a review of the empirical literature. *Review of Economics*, *72*, 213–228.
- Carriero, A., Clark, T. E., & Marcellino, M. (2018). Measuring uncertainty and its impact on the economy. *Review of Economics and Statistics*, *100*, 799–815.
- Challu, C., Kang, Y., Santos, J., Montero-Manso, P., & Hyndman, R. J. (2023). Nhits: Neural hierarchical interpolation for time series forecasting. Preprint, available online.
- Chevallier, J. (2011). Evaluating the carbon-macroeconomy relationship: Evidence from threshold vector error-correction and markov-switching var models. *Economic Modelling*, *28*, 2634–2656.
- Cho, C., Yang, J., & Jang, B. (2024). Climate policy uncertainty and its impact on real estate market dynamics: A sectoral and regional analysis. *PloS one*, *19*, e0311688.
- Danisman, G. O., Bilyay-Erdogan, S., & Demir, E. (2025). Economic uncertainty and climate change exposure. *Journal of Environmental Management*, *373*, 123760.
- Dogan, E., & Turkekul, B. (2016). Co 2 emissions, real output, energy consumption, trade, urbanization and financial development: testing the ekc hypothesis for the usa. *Environmental Science and Pollution Research*, *23*, 1203–1213.
- Drews, S., & Van den Bergh, J. C. (2016). What explains public support for climate policies? a review of empirical and experimental studies. *Climate policy*, *16*, 855–876.
- Durbin, J., & Koopman, S. J. (2002). A simple and efficient simulation smoother for state space time series analysis. *Biometrika*, *89*, 603–615.
- Ehm, W., Gneiting, T., Jordan, A., & Krüger, F. (2016). Of quantiles and expectiles: consistent scoring functions, choquet representations and forecast rankings. *Journal of the Royal Statistical Society Series B: Statistical Methodology*, *78*, 505–562.
- Fankhauser, S., & Tol, R. S. (2005). On climate change and economic growth. *Resource and Energy Economics*, *27*, 1–17.
- Faraway, J. J. (1998). *Time Series Modeling with Applications in R*. CRC Press.
- Frayser, L. (2021). India pledges net-zero emissions by 2070—but also wants to expand coal mining, .
- Gaies, B. (2025). Sino-american spillovers in climate policy uncertainty and financial instability: A time-varying quantile network analysis. *Journal of Environmental Management*, *386*, 125746.
- Gavriilidis, K. (2021). Measuring climate policy uncertainty. *Available at SSRN 3847388*, .
- Ge, J., & Lin, B. (2021). Impact of public support and government’s policy on climate change in china. *Journal of Environmental Management*, *294*, 112983.
- Ghani, U., Zhu, B., Qin, Q., & Ghani, M. (2024). Forecasting us stock market volatility: evidence from esg and cpu indices. *Finance Research Letters*, *59*, 104811.
- Giovanardi, F., & Kaldorf, M. (2024). Pro-cyclical emissions and optimal monetary policy. *Available at SSRN 4802492*, .

- Granger, C. W. (1969). Investigating causal relations by econometric models and cross-spectral methods. *Econometrica: journal of the Econometric Society*, (pp. 424–438).
- Granger, C. W. J., & Joyeux, R. (1980). An introduction to long-memory time series models and fractional differencing. *Journal of Time Series Analysis*, 1, 15–29.
- Grinsted, A., Moore, J. C., & Jevrejeva, S. (2004). Application of the cross wavelet transform and wavelet coherence to geophysical time series. *Nonlinear Processes in Geophysics*, 11, 561–566.
- Grossman, G. M., & Krueger, A. B. (1995). Economic growth and the environment. *The quarterly journal of economics*, 110, 353–377.
- Halkos, G. E., & Paizanos, E. A. (2016). The effects of fiscal policy on co2 emissions: evidence from the usa. *Energy policy*, 88, 317–328.
- Heutel, G. (2012). How should environmental policy respond to business cycles? optimal policy under persistent productivity shocks. *Review of Economic Dynamics*, 15, 244–264.
- Hyndman, R. J., & Athanasopoulos, G. (2018). *Forecasting: principles and practice*. OTexts.
- Ide, T. (2020). Recession and fossil fuel dependence undermine climate policy commitments. *Environmental Research Communications*, 2, 101002.
- Iqbal, N., Bouri, E., Shahzad, S. J. H., & Alsagr, N. (2024). Asymmetric impacts of chinese climate policy uncertainty on chinese asset prices. *Energy Economics*, 133, 107518.
- Jordà, Ò. (2005). Estimation and inference of impulse responses by local projections. *American economic review*, 95, 161–182.
- Khan, H., Metaxoglou, K., Knittel, C. R., & Papineau, M. (2019). Carbon emissions and business cycles. *Journal of Macroeconomics*, 60, 1–19.
- Koning, A. J., Franses, P. H., Hibon, M., & Stekler, H. O. (2005). The m3 competition: Statistical tests of the results. *International Journal of Forecasting*, 21, 397–409.
- Koop, G., Korobilis, D. et al. (2010). Bayesian multivariate time series methods for empirical macroeconomics. *Foundations and Trends® in Econometrics*, 3, 267–358.
- Kuznets, S. (1955). Economic growth and income inequality. *The American Economic Review*, 45, 1–28.
- Layzer, J. A. (2011). chapter 8 cold front: how the recession stalled obama’s clean-energy agenda. *Reaching for a New Deal: Ambitious Governance, Economic Meltdown, and Polarized Politics in Obama’s First Two Years*, (p. 321).
- Le, A. H. (2025). Climate change and carbon policy: A story of optimal green macroprudential and capital flow management. *Energy Economics*, (p. 108501).
- Liang, C., Umar, M., Ma, F., & Huynh, T. L. D. (2022). Climate policy uncertainty and world renewable energy index volatility forecasting. *Technological Forecasting & Social Change*, 182, 121810.
- Lu, F., Ma, F., & Feng, L. (2024). Carbon dioxide emissions and economic growth: New evidence from gdp forecasting. *Technological Forecasting and Social Change*, 205, 123464.
- Matzner, A., & Steininger, L. (2024). Firms’ heterogeneous (and unintended) investment response to carbon price increases, .
- McCracken, M. W., & Ng, S. (2016). Fred-md: A monthly database for macroeconomic research. *Journal of Business & Economic Statistics*, 34, 574–589.
- Michaelowa, A., & Michaelowa, K. (2015). Do rapidly developing countries take up new responsibilities for climate change mitigation? *Climatic Change*, 133, 499–510.
- Michalowicz, J. V., Nichols, J. M., & Bucholtz, F. (2013). *Handbook of differential entropy*. Crc Press.
- Miranda-Agrippino, S., & Rey, H. (2020). Us monetary policy and the global financial cycle. *The Review of Economic Studies*, 87, 2754–2776.
- Mokni, K., Zaier, L. H., Youssef, M., & Jabeur, S. B. (2024). Quantile connectedness between the climate policy and economic uncertainty: Evidence from the g7 countries. *Journal of Environmental Management*, 351, 119826.
- Moramarcò, G. (2024). Financial-cycle ratios and medium-term predictions of gdp: Evidence from the united states. *International Journal of Forecasting*, 40, 777–795.
- Naifar, N. (2024). Spillover among sovereign credit risk and the role of climate uncertainty. *Finance Research Letters*, 61, 104935.
- Narayan, P. K., Saboori, B., & Soleymani, A. (2016). Economic growth and carbon emissions. *Economic Modelling*, 53, 388–397.
- Newell, R. G., Prest, B. C., & Sexton, S. E. (2021). The gdp-temperature relationship: implications for climate change damages. *Journal of Environmental Economics and Management*, 108, 102445.
- Newey, W. K., & West, K. D. (1987). Hypothesis testing with efficient method of moments estimation. *International Economic Review*, (pp. 777–787).

- Ng, C.-F., Yii, K.-J., Lau, L.-S., & Go, Y.-H. (2023). Unemployment rate, clean energy, and ecological footprint in oecd countries. *Environmental Science and Pollution Research*, *30*, 42863–42872.
- Obani, P. C., & Gupta, J. (2016). The impact of economic recession on climate change: eight trends. *Climate and Development*, *8*, 211–223.
- Oreshkin, B. N., Carпов, D., Chapados, N., & Bengio, Y. (2019). N-beats: Neural basis expansion analysis time series forecasting. In *International Conference on Learning Representations (ICLR)*.
- Pei, Z., Chen, X., Li, X., Liang, J., Lin, A., Li, S., Yang, S., Bin, J., & Dai, S. (2022). Impact of macroeconomic factors on ozone precursor emissions in china. *Journal of Cleaner Production*, *344*, 130974.
- Rad, H., Low, R. K. Y., Miffre, J., & Faff, R. (2023). The commodity risk premium and neural networks. *Journal of Empirical Finance*, *74*, 101433.
- Raza, S. A., Khan, K. A., Benkraiem, R., & Guesmi, K. (2023). The importance of climate policy uncertainty in forecasting the green, clean and sustainable financial markets volatility. *Journal of Sustainable Finance & Investment*, .
- Ruhlemann, M., & Schulz, F. (2020). Wavelet coherence between economic policy uncertainty and stock markets in major economies. *Applied Economics Letters*, *27*, 1243–1248.
- Rumelhart, D. E., Hinton, G. E., & Williams, R. J. (1986). Learning internal representations by error propagation. In *Parallel Distributed Processing: Explorations in the Microstructure of Cognition* (pp. 318–362). MIT Press volume 1.
- von Schneidemesser, E., Monks, P. S., Allan, J. D., Bruhwiler, L., Forster, P., Fowler, D., Lauer, A., Morgan, W. T., Paasonen, P., Righi, M., Sindelarova, K., & Sutton, M. A. (2015). Chemistry and the linkages between air quality and climate change. *Chemical Reviews*, *115*, 3856–3897.
- Schreiber, T. (2000). Measuring information transfer. *Physical review letters*, *85*, 461.
- Scott, S. L., & Varian, H. R. (2014). Predicting the present with bayesian structural time series. *International Journal of Mathematical Modelling and Numerical Optimisation*, *5*, 4–23.
- Shahbaz, M., Balsalobre-Lorente, D., & Sinha, A. (2019). Foreign direct investment–co2 emissions nexus in middle east and north african countries: Importance of biomass energy consumption. *Journal of cleaner production*, *217*, 603–614.
- Shannon, C. E. (1948). A mathematical theory of communication. *The Bell system technical journal*, *27*, 379–423.
- Shum, R. Y. (2012). Effects of economic recession and local weather on climate change attitudes. *Climate Policy*, *12*, 38–49.
- Sobrino, N., & Monzon, A. (2014). The impact of the economic crisis and policy actions on ghg emissions from road transport in spain. *Energy Policy*, *74*, 486–498.
- Sultanuzzaman, M. R., Yahya, F., & Lee, C.-C. (2024). Exploring the complex interplay of green finance, business cycles, and energy development. *Energy*, *306*, 132479.
- Vacha, L., & Barunik, J. (2012). Co-movement of energy commodities revisited: Evidence from wavelet coherence analysis. *Energy Economics*, *34*, 241–247.
- Varian, H. R. (2014). Big data: New tricks for econometrics. *Journal of Economic Perspectives*, *28*, 3–28.
- Wang, Q., & Wang, S. (2019). Decoupling economic growth from carbon emissions growth in the united states: The role of research and development. *Journal of Cleaner Production*, *234*, 702–713.
- West, M., & Harrison, J. (1997). *Bayesian Forecasting and Dynamic Models*. Springer.
- Wu, G., & Hu, G. (2024). Asymmetric spillovers and resilience in physical and financial assets amid climate policy uncertainties: Evidence from china. *Technological Forecasting and Social Change*, *208*, 123701.
- Wu, J., Yang, C., & Chen, L. (2024). Examining the non-linear effects of monetary policy on carbon emissions. *Energy Economics*, *131*, 107206.
- Wu, Z., Huang, X., Chen, R., Mao, X., & Qi, X. (2022). The united states and china on the paths and policies to carbon neutrality. *Journal of Environmental Management*, *320*, 115785.
- Xing, X., Liu, Y., Zhu, Y., & Deng, J. (2024). The impact of climate policy uncertainty on china’s green energy and non-ferrous metals market co-movement: Evidence from spillover perspectives. *Journal of Environmental Management*, *367*, 121845.
- Xu, Y., Li, M., Yan, W., & Bai, J. (2022). Predictability of the renewable energy market returns: The informational gains from the climate policy uncertainty. *Resources Policy*, *79*, 103141.
- Yang, J., Dong, D., & Liang, C. (2024). Climate policy uncertainty and the u.s. economic cycle. *Technological Forecasting & Social Change*, *202*, 123344.
- Yeganeh, A. J., McCoy, A. P., & Schenk, T. (2020). Determinants of climate change policy adoption: A meta-analysis. *Urban Climate*, *31*, 100547.
- Yousaf, I., Mohammed, K. S., Yousaf, U. B., & Serret, V. (2025). The effect of crypto price fluctuations on crypto

- mining, and co2 emissions amid geopolitical risk. *Finance Research Letters*, 72, 106551.
- Zeng, Y., Liu, L., Li, X., Wei, Y., & Hong, Y. (2023). Transformers in time series: A survey. *IEEE Transactions on Neural Networks and Learning Systems*, .
- Zhang, P. (2023). Environmental policy and carbon emissions in business cycles with public infrastructure investment. *Journal of Cleaner Production*, 384, 135670.
- Zhang, R. J., & Razzaq, A. (2022). Influence of economic policy uncertainty and financial development on renewable energy consumption in the bricst region. *Renewable Energy*, 201, 526–533.
- Zhang, W., & Chiu, Y.-B. (2020). Do country risks influence carbon dioxide emissions? a non-linear perspective. *Energy*, 206, 118048.
- Ziegel, J. F., Krüger, F., Jordan, A., & Fasciati, F. (2017). Murphy diagrams: Forecast evaluation of expected shortfall. *arXiv preprint arXiv:1705.04537*, .

8. Appendix

8.1. Causal Analysis

This section investigates the causal impact of several macroeconomic and financial cycle variables on the US Climate Policy Uncertainty (CPU) index. To identify the most influential predictors, we employ four methods: Transfer Entropy, Granger Causality, Cross-Correlation, and Wavelet Coherence. These approaches enable us to capture linear and nonlinear dependencies, as well as time-varying and frequency-specific relationships between the CPU index and the candidate explanatory variables.

8.1.1. Transfer Entropy

Information entropy was first introduced by [Shannon, 1948](#). This concept is central to measuring the amount of uncertainty or information contained in a system. Within the framework of Shannon’s theory, for a coupled system (X, Y) , where $P_Y(y)$ is the probability density function (pdf) of the random variable Y , and $P_{X,Y}$ is the joint pdf of X and Y , the joint entropy between X and Y is defined as:

$$H(X, Y) = - \sum_{x \in X} \sum_{y \in Y} P_{X,Y}(x, y) \log(P_{X,Y}(x, y)).$$

The conditional entropy is given by $H(Y | X) = H(X, Y) - H(X)$. It can be interpreted as the uncertainty in Y given the knowledge of a specific value of X . The Transfer Entropy, as introduced by [Schreiber, 2000](#), has been proven to be an effective tool in identifying causal relationships in nonlinear systems. It captures the directional flow of information between systems without the need for a predefined functional form of interaction. The Transfer Entropy is defined as the difference between two conditional entropies:

$$TE(X \rightarrow Y | Z) = H(Y^F | Y^P, Z^P) - H(Y^F | X^P, Y^P, Z^P),$$

where Y^F is the forward time-shifted version of Y at lag Δt with respect to past values of X^P , Y^P , and Z^P . This may also be expressed as a sum of Shannon entropies:

$$TE(X \rightarrow Y) = H(Y^P, X^P) - H(Y^F, Y^P, X^P) + H(Y^F, Y^P) - H(Y^P).$$

Since Transfer Entropy is an asymmetric measure, that is, $TE(X \rightarrow Y) \neq TE(Y \rightarrow X)$, it can be used to quantify the direction of information flow between systems. The Net Information Flow is defined as:

$$\hat{TE}_{X \rightarrow Y} = TE_{X \rightarrow Y} - TE_{Y \rightarrow X}.$$

This quantity indicates the dominant direction of information flow, with a positive value signifying that X provides more predictive information about Y than Y does about X ([Michalowicz, Nichols & Bucholtz, 2013](#)).

8.1.2. Granger Causality

The Granger causality test is widely used for analyzing predictive power between different time series. [Granger, 1969](#) defined Granger causality as the ability to predict future values of the variable Y using past values of both X and Y . In this framework, X is said to Granger-cause Y if the inclusion of past values of X improves the prediction of Y . Let X_t and Y_t be random variables at time t , and let X_t, Y_t, Z_t represent three stochastic processes. Define \hat{Y}_{t+1} as the predictor of Y at time $t + 1$. We evaluate the expected value

of a loss function $g(e)$, where the error is $e = \hat{Y}_{t+1} - Y_{t+1}$, for both models. Typically, the forms of g include the L_1 or L_2 norms, and the functions f_1 and f_2 minimize the expected value of the loss function:

$$\begin{aligned} R(Y_{t+1} | Y_t, Z_t) &= \mathbb{E}[g(Y_{t+1} - f_1(Y_t, Z_t))] \\ R(Y_{t+1} | X_t, Y_t, Z_t) &= \mathbb{E}[g(Y_{t+1} - f_2(X_t, Y_t, Z_t))]. \end{aligned}$$

Definition 1. X does not G -cause Y relative to the additional information Z if and only if:

$$R(Y_{t+1}|X_t, Y_t, Z_t) = R(Y_{t+1}|Y_t, Z_t).$$

The classical Granger test is implemented via vector autoregressive (VAR(p)) model, where p is the number of lagged observations:

$$\begin{aligned} Y(t) &= \alpha + \sum_{\Delta t=1}^p \beta_{\Delta t} Y(t - \Delta t) + \epsilon_t, \\ Y(t) &= \hat{\alpha} + \sum_{\Delta t=1}^p \hat{\beta}_{\Delta t} Y(t - \Delta t) + \sum_{\Delta t=1}^p \hat{\gamma}_{\Delta t} X(t - \Delta t) + \hat{\epsilon}_t, \end{aligned}$$

By Definition 1, X does not G -cause Y if and only if the prediction errors from the restricted and unrestricted models are equal. A one-way ANOVA test can be used to assess if the residuals differ significantly. The null hypothesis H_0 asserts that $(\gamma_1, \gamma_2, \dots, \gamma_p)$ are jointly zero, rejecting H_0 indicates that X Granger-cause Y .

8.1.3. Cross-Correlation

Cross-correlation is a fundamental tool in time series analysis used to examine the linear relationship between two stochastic processes at different time lags. The cross-correlation function between two stationary time series X_t and Y_t is defined as:

$$\rho_{XY}(k) = \frac{\mathbb{E}[(X_{t-k} - \mu_X)(Y_t - \mu_Y)]}{\sigma_X \sigma_Y},$$

where k represents the time lag, and $\mu_X, \mu_Y, \sigma_X, \sigma_Y$ denote the means and standard deviations of X and Y , respectively. The cross-correlation function provides a quantitative measure of the strength and direction of the linear relationship between the two series at each lag k . Significant cross-correlation at nonzero lags may suggest potential causality or feedback mechanisms, though the method does not imply directionality. Cross-correlation analysis is frequently employed in econometrics and environmental sciences to explore temporal dependencies, particularly when evaluating synchronized behaviour or transmission effects between macroeconomic and environmental indicators. However, it is limited to linear dependencies and may not adequately capture nonlinear or nonstationary relationships (Box, Jenkins, Reinsel & Ljung, 2015).

8.1.4. Wavelet Coherence

Wavelet coherence is a powerful tool for examining localized correlation and phase relationships between two nonstationary time series across time and frequency domains. Unlike classical spectral approaches, wavelet coherence captures transient associations by decomposing the signals using continuous wavelet transforms. The continuous wavelet transform of a signal $X(t)$ with respect to a mother wavelet ψ is defined as:

$$W^X(a, b) = \int_{-\infty}^{\infty} X(t) \frac{1}{\sqrt{a}} \bar{\psi} \left(\frac{t-b}{a} \right) dt,$$

where a is the scale (inversely proportional to frequency), b is the translational value, and $\bar{\cdot}$ represents the operation of complex conjugation. The cross-wavelet transform between two signals $X(t)$ and $Y(t)$ is given by:

$$W^{XY}(a, b) = W^X(a, b) W^{\bar{Y}}(a, b).$$

The wavelet coherence is then defined as:

$$R^2(a, b) = \frac{|S(a^{-1}W^{XY}(a, b))|^2}{S(a^{-1}|W^X(a, b)|^2) \cdot S(a^{-1}|W^Y(a, b)|^2)},$$

where S is a smoothing operator in time and scale. The resulting measure $R^2(a, b) \in [0, 1]$ reflects the local linear correlation between X and Y at each time-scale location (a, b) (Grinsted, Moore & Jevrejeva, 2004). Wavelet coherence is especially suitable for analyzing nonstationary and multiscale relationships in economic and environmental time series, where the interactions may vary across frequencies and evolve over time (Vacha & Barunik, 2012; Ruhlemann & Schulz, 2020).

8.1.5. Results of Causal Analyses

We implement the four causal inference approaches: Transfer Entropy, Granger Causality, Cross-Correlation, and Wavelet Coherence, to examine the potential causal relationships between the CPU index and 137 macroeconomic and financial cycle variables, as well as the Google Trends data. Tables 7 and 8 summarize the results, where a “Y” indicates statistically significant evidence of causality, while an “N” denotes the absence of such evidence.

Table 7: Presents the complete results of statistical tests for the macroeconomic and financial cycle variables.

Variables	Description	TE	GC	CC	W
AAA	Moody’s Seasoned Aaa Corporate Bond Yield	Y	N	N	N
AAAFFM	Moody’s Aaa Corporate Bond Minus FEDFUNDS	N	N	N	N
AMDMNOx	New Orders for Durable Goods	N	N	N	Y
AMDMUOx	Unfilled Orders for Durable Goods	N	N	N	Y
ANDENOx	New Orders for Nondefense Capital Goods	N	N	N	Y
AWHMAN	New Orders for Nondefense Capital Goods	N	N	Y	Y
AWOTMAN	Average Weekly Overtime Hours : Manufacturing	N	N	N	Y
BAA	Moody’s Seasoned Baa Corporate Bond Yield	Y	N	N	Y
BAAFFM	Moody’s Baa Corporate Bond Minus FEDFUNDS	N	N	N	Y
BCI	Business Confidence Index	Y	N	Y	Y
BOGMBASE	Board of Governors Monetary Base	N	N	N	Y
BUSINVx	Total Business Inventories	Y	N	Y	Y
BUSLOANS	Commercial and Industrial Loans	N	Y	N	Y
CAPE	Cyclically Adjusted Price/Earnings ratio	Y	N	Y	Y
CAPR	Cyclically Adjusted Price/Rent ratio	Y	Y	Y	Y
CE16OV	Civilian Employment	N	N	Y	Y
CES0600000007	Average Weekly Hours: Goods-Producing	N	N	Y	Y
CES0600000008	Average Hourly Earnings: Goods-Producing	N	Y	N	Y
CES1021000001	All Employees: Mining and Logging: Mining	N	N	N	Y
CES2000000008	Average Hourly Earnings: Construction	Y	Y	N	Y
CES3000000008	Average Hourly Earnings: Manufacturing	N	N	N	Y

Continued on next page

Table 7 – continued from previous page

Variables	Full Form	TE	GC	CC	W
CLAIMSx	Initial Claims	N	Y	N	Y
CLF16OV	Civilian Labor Force	N	Y	N	Y
CLI	Composite Leading Indicator	N	N	Y	Y
CMRMTSPLx	Real Manufacturing and Trade Industries Sales	N	N	N	Y
COMPAPFFx	3-Month Commercial Paper Minus FEDFUNDS	N	N	Y	Y
CONSPI	Nonrevolving consumer credit to Personal Income	N	Y	N	Y
CP3Mx	3-Month AA Financial Commercial Paper Rate	N	N	Y	Y
CPIAPPSL	CPI : Apparel	N	N	N	Y
CPIAUCSL	CPI : All Items	N	N	N	Y
CPIMEDSL	CPI : Medical Care	N	N	N	Y
CPITRNSL	CPI : Transportation	N	Y	N	Y
CPIULFSL	CPI : All Items Less Food	N	N	N	Y
CRED	Credit/GDP ratio	N	Y	Y	Y
CRED_GDP	Credit/GDP ratio	Y	Y	Y	Y
CUMFNS	Manufacturing capacity utilization	N	Y	Y	Y
CUUR0000SA0L2	CPI : All items less shelter	N	N	N	Y
CUSR0000SA0L5	CPI : All items less medical care	N	N	N	Y
CUSR0000SAC	CPI: Commodities	N	N	N	Y
CUUR0000SAD	CPI: Durables	Y	N	N	Y
CUSR0000SAS	CPI: Services	N	N	N	Y
DDURRG3M086SBEA	Personal Consumption Expenditures: Durable Goods	Y	Y	N	Y
DMANEMP	All Employees: Durable goods	N	Y	Y	Y
DNDGRG3M086SBEA	Personal Consumption Expenditures: Nondurable Goods	N	N	N	Y
DPCERA3M086SBEA	Real Personal Consumption Expenditure	Y	N	N	Y
DSERRG3M086SBEA	Personal Consumption Expenditures: Services	N	N	N	Y
DTCOLNVHFNM	Consumer Motor Vehicle Loans Outstanding	N	Y	N	Y
DTCTHFNM	Total Consumer Loans and Leases Outstanding	N	Y	N	N
EXCAUSx	Canada/US Foreign Exchange Rate	N	N	N	Y
EXJPUSx	Japan/US Foreign Exchange Rate	N	N	N	N
EXSZUSx	Switzerland/US Foreign Exchange Rate	N	N	N	Y
EXUSUKx	US/UK Foreign Exchange Rate	N	N	N	N
FEDFUNDS	Effective Federal Funds Rate	N	N	Y	Y
GS1	1-Year Treasury Rate	Y	N	Y	Y
GS5	5-Year Treasury Rate	N	N	N	Y
GS10	10-Year Treasury Rate	N	N	N	Y
HOUST	Housing Starts: Total New Privately Owned	Y	N	N	Y
HOUSTMW	Housing Starts, Midwest	N	N	Y	Y
HOUSTNE	Housing Starts, Northeast	N	Y	Y	Y
HOUSTS	Housing Starts, South	Y	Y	N	Y
HOUSTW	Housing Starts, West	Y	N	N	Y
HPI	House Price Index	Y	N	Y	Y
HWI	Help-Wanted Index for United States	N	Y	Y	Y
HWIURATIO	Ratio of Help Wanted/Number of Unemployed	Y	Y	Y	Y
INDPRO	Industrial Production (IP) Index	N	Y	N	Y
INVEST	Securities in Bank Credit at All Commercial Banks	N	N	N	N
IPB51222S	IP: Residential Utilities	N	Y	N	Y
IPBUSEQ	IP: Business Equipment	N	N	N	Y

Continued on next page

Table 7 – continued from previous page

Variables	Full Form	TE	GC	CC	W
IPCONGD	IP: Consumer Goods	N	N	N	Y
IPDCONGD	IP: Durable Consumer Goods	N	N	N	Y
IPDMAT	IP: Durable Materials	N	N	N	Y
IPFINAL	IP: Final Products (Market Group)	N	N	N	Y
IPFPNSS	IP: Final Products and Nonindustrial Supplies	N	N	N	Y
IPFUELS	IP: Fuels	N	N	N	Y
IPMANSICS	IP: Manufacturing (SIC)	N	Y	N	Y
IPMAT	IP: Materials	N	Y	N	Y
IPNCONGD	IP: Nondurable Consumer Goods	N	N	N	Y
IPNMAT	IP: Nondurable Materials	Y	Y	N	Y
ISRATIOx	Total Business: Inventories to Sales Ratio	N	N	N	Y
M1SL	M1 Money Stock	N	Y	N	Y
M2REAL	Real M2 Money Stock	Y	N	Y	Y
M2SL	M2 Money Stock	N	N	N	Y
MANEMP	All Employees: Manufacturing	Y	N	Y	Y
Mortg	Household Real Mortgage Debt Growth	N	N	N	Y
Mortg/Income	Household Mortgage/Income ratio	N	Y	N	Y
NDMANEMP	All Employees: Nondurable goods	Y	N	Y	Y
NFEI	Chicago Fed national financial condition index	N	Y	N	Y
NONBORRES	Reserves Of Depository Institutions	N	N	N	Y
NONREVSL	Total Nonrevolving Credit	N	Y	N	Y
OILPRICEx	Crude Oil, spliced WTI and Cushing	N	N	N	Y
PAYEMS	All Employees: Total nonfarm	Y	N	Y	Y
PCEPI	Personal Consumption Expenditures: Chain Index	N	N	N	Y
PERMIT	New Private Housing Permits (SAAR)	Y	N	N	Y
PERMITMW	New Private Housing Permits, Midwest (SAAR)	N	N	N	Y
PERMITNE	New Private Housing Permits, Northeast (SAAR)	Y	N	Y	Y
PERMITS	New Private Housing Permits, South (SAAR)	N	N	Y	Y
PERMITW	New Private Housing Permits, West (SAAR)	N	N	N	Y
PIP/Income	Personal Interest Payments/Income ratio	Y	N	Y	Y
PPICMM	PPI: Metals and metal products:	N	N	N	Y
PRFI/GDP	Private Residential Fixed Investment/GDP ratio	N	Y	Y	Y
REALLN	Real Estate Loans at All Commercial Banks	N	N	N	Y
RETAILx	Retail and Food Services Sales	N	N	N	Y
RPI	Real Personal Income	N	Y	N	Y
S&P.500	S&P's Common Stock Price Index: Composite	N	N	N	Y
S&P.div.yield	S&P's Composite Common Stock: Dividend Yield	N	N	N	Y
S&P.PE.ratio	S&P's Composite Common Stock: Price/Earnings Ratio	N	N	N	Y
SP500	Real S&P500 Index Growth	N	N	N	Y
SRVPRD	All Employees: Service-Providing Industries	Y	Y	Y	Y
T10YFFM	10-Year Treasury C Minus FEDFUNDS	N	N	Y	Y
T1YFFM	1-Year Treasury C Minus FEDFUNDS	Y	N	Y	Y
T5YFFM	5-Year Treasury C Minus FEDFUNDS	N	N	Y	Y
TB3MS	3-Month Treasury Bill	N	N	Y	Y
TB3SMFFM	3-Month Treasury C Minus FEDFUNDS	Y	N	Y	Y
TB6MS	6-Month Treasury Bill	Y	N	Y	Y
TB6SMFFM	6-Month Treasury C Minus FEDFUNDS	Y	N	Y	Y

Continued on next page

Table 7 – continued from previous page

Variables	Full Form	TE	GC	CC	W
TOTRESNS	Total Reserves of Depository Institutions	N	N	N	Y
UEMP15OV	Civilians Unemployed - 15 Weeks & Over	Y	Y	N	Y
UEMP15T26	Civilians Unemployed for 15-26 Weeks	Y	Y	N	Y
UEMP27OV	Civilians Unemployed for 27 Weeks & Over	N	N	N	Y
UEMP5TO14	Civilians Unemployed for 5-14 Weeks	N	Y	N	Y
UEMPLT5	Civilians Unemployed for Less than 5 Weeks	N	N	N	Y
UEMPMEAN	Average Duration of Unemployment (Weeks)	Y	Y	N	Y
UMCSENTx	Consumer Sentiment Index	Y	N	N	Y
UNRATE	Civilian Unemployment Rate	Y	Y	Y	Y
USCONS	All Employees: Construction	N	N	N	Y
USFIRE	All Employees: Financial Activities	Y	N	N	Y
USGOOD	All Employees: Goods-Producing Industries	N	N	Y	Y
USGOVT	All Employees: Government	Y	N	N	Y
USTPU	All Employees: Trade, Transportation & Utilities	Y	N	Y	Y
USTRADE	All Employees: Retail Trade	Y	N	Y	Y
USWTRADE	All Employees: Wholesale Trade	Y	N	Y	Y
VIXCLSx	Cboe Volatility Index	N	N	N	Y
W875RX1	Real Personal Income Excluding Transfer Receipts	Y	Y	N	Y
WPSFD49207	PPI by Commodity: Finished Goods series	N	Y	N	Y
WPSFD49502	PPI by Commodity: Personal Consumption Goods	N	Y	N	Y
WPSID61	PPI by Commodity Type: Processed Goods	N	N	N	Y
WPSID62	PPI by Commodity Type: Unprocessed Goods	N	N	N	Y

Note: TE = Transfer Entropy, GC = Granger Causality, CC = Cross-Correlation, W = Wavelet Coherence.

Table 8: Presents the complete results of statistical tests for Google Trends covariates.

Search Terms	Description	TE	GC	CC	W
Carbon Credits: (Worldwide)	Tradable credits to emit CO ₂ .	Y	N	Y	N
Carbon Emissions: (Worldwide)	Total release of CO ₂ into the atmosphere.	Y	Y	Y	Y
Carbon Footprint: (Worldwide)	Individual or firm emissions.	Y	N	Y	Y
Carbon Tax: (Worldwide)	Taxes on carbon emissions.	Y	Y	Y	Y
Clean Energy: (Worldwide)	Energy generated from renewable sources.	Y	Y	Y	Y
Climate Action: (Worldwide)	Measures to mitigate climate change.	Y	Y	Y	Y
Climate News: (Worldwide)	Media coverage on climate change.	Y	Y	Y	Y
Climate Policy: (Worldwide)	Policies addressing climate change.	Y	Y	Y	Y
Climate Risk: (Worldwide)	Risks arising from climate-related events.	Y	Y	Y	Y
Climate Technology: (Worldwide)	Technology reducing GHG emissions.	Y	Y	Y	Y
Electric Vehicle: (Worldwide)	Battery-powered vehicles.	Y	N	Y	Y
Energy Efficiency: (Worldwide)	Using less energy to perform the same task.	Y	N	Y	Y
Energy Policy: (Worldwide)	Regulations on energy consumption.	Y	Y	Y	Y
Energy Transition: (Worldwide)	Shift from fossil fuel to renewable sources.	Y	Y	Y	Y
Environmental Policy: (Worldwide)	Policies addressing environmental issues.	Y	N	Y	Y
Environmental Tax: (Worldwide)	Taxes on harmful activities.	Y	Y	Y	Y
Global Warming Policy: (Worldwide)	Policies to limit temperature rise.	Y	N	Y	Y
Green Finance: (Worldwide)	Investments promoting sustainability.	Y	N	Y	Y

Continued on next page

Table 8 – continued from previous page

Search Terms	Description	TE	GC	CC	W
Green Infrastructure: (Worldwide)	Sustainable urban planning.	Y	Y	Y	Y
Green Jobs: (Worldwide)	Employment in sustainable sectors.	Y	N	Y	Y
Green Technology: (Worldwide)	Technology reducing environmental harm.	Y	N	Y	Y
Greenhouse Gas Emissions: (Worldwide)	Emissions of CO ₂ , CH ₄ , and N ₂ O.	Y	Y	Y	Y
Greenwashing: (Worldwide)	False sustainability claims.	Y	Y	Y	Y
Renewable Energy: (Worldwide)	Energy from natural sources.	Y	N	Y	Y
Sustainability: (Worldwide)	Using resources wisely.	Y	Y	Y	Y
Sustainable Development: (Worldwide)	Economic growth with sustainability.	Y	Y	Y	Y
Sustainable Development Goals: (Worldwide)	UN-adopted framework of 17 goals.	Y	N	Y	Y
Sustainable Living: (Worldwide)	Lifestyle reducing environmental impact.	Y	N	Y	Y
UN Climate Conference: (Worldwide)	Annual international climate summit.	Y	N	Y	Y
Zero Emissions: (Worldwide)	Completely eliminating GHG emissions.	Y	Y	Y	Y

Note: TE = Transfer Entropy, GC = Granger Causality, CC = Cross-Correlation, W = Wavelet Coherence.